The effect of resolution and diffusion on the Simulated climate

by

J.F. Dyson

DCTN 33 November 1985

DYNAMICAL CLIMATOLOGY TECHNICAL NOTE NO. 33

THE EFFECT OF RESOLUTION AND DIFFUSION ON THE SIMULATED CLIMATE

by

J F Dyson

Met O 20 (Dynamical
Climatology Branch)
Meteorological Office
London Road
Bracknell
Berkshire, U.K. RG12 2SZ

November 1985

Note: This paper has not been published. Permission to quote from it should be obtained from the Assistant Director of the above Meteorological Office Branch.

KW/39

The effect of resolution and diffusion on the simulated climate

by J. F. Dyson

1. Introduction

Various authors have studied the effects of resolution and diffusion on both short range forecasts and climate simulation. Williamson (1978) investigated a series of 5 day integrations using the NCAR grid point model, with differing resolutions and amounts of diffusion. Manabe et al (1970) studied two resolutions, 500 km and 250 km, of a grid point model but for longer, 'climate type', integrations. More recently Manabe, Hahn and Holloway (1978; hereafter MHH) compared three different spectral resolutions. A result common to all these papers is that when the resolution is increased from around 500 km to 250 km there is a significant and realistic increase in the eddy activity. Williamson attributed this to a better simulation of the growth rates of baroclinic waves due mainly to the decrease of lateral eddy viscosity - taken to vary like the square of the grid size - when the resolution is increased. An analytical study by Merilees (1975) confirmed that there is a significant improvement in the growth rate of baroclinic waves when the resolution is increased and that most of the improvement can be attributed to the decrease in eddy viscosity.

The emphasis of this study is the effect of resolution and diffusion in a general circulation model on the simulated climate. In respect of the effect of resolution this is akin to the investigation of MHH. Two resolutions were considered, 5° x 7.5° and 2.5° x 3.75° (approximately 550 km and 275 km north south grid spacing respectively) on a regular latitude longitude grid, referred to as coarse and medium resolution respectively. Experience has shown that (for the non-linear formulation used) at a given resolution the best simulation is obtained by using the minimum diffusion constant which maintains stability (as we shall see, this conclusion is less definite at the coarse resolution); this minimum is found to vary, roughly, with the square of the grid length. Comparing the coarse and

medium resolution models, with the minimum diffusion constant at each resolution, it is found that for perpetual July simulations there is an overall improvement with increased resolution. However in a perpetual January simulation, in the Northern hemisphere the coarse resolution simulation is superior. A possible explanation of this is put forward. Another January simulation using the medium resolution model, with the same diffusion constant as used in the coarse resolution model, is studied in order to separate the effect of changing resolution from that of changing the diffusion constant. In agreement with the findings of Williamson and Merilees, it is shown that most of the difference in eddy kinetic energy at differing resolution can be attributed to the change in diffusion constant. However, it is found that not all the differences can be attributed to the change in diffusion constant.

2. The January Integrations

Four integrations are considered in order to elucidate

1) the effect of resolution
2) the effect of changing the diffusion constant

Each of these integrations was run for 60 days with fixed SST's, sea-ice extents and radiation conditions for January. The initial conditions for all four experiments were derived from day 1 of an old IBM experiment HGC4 (whose initial conditions, in turn, were based on hand analysed data from 12 GMT on 27th December 1972). All the integrations had the same physical parametrizations, that is a boundary scheme based on Clarke (1970), a 'climatological' radiation scheme (zonally prescribed solar heating rates and a simple infra red cooling scheme) and a penetrative convection scheme (Lyne and Rowntree 1976). The horizontal diffusion or lateral eddy viscosity is a non-linear diffusion formulation, specifically a modification of

$$\lambda \, |\nabla^2\phi| \, \nabla^2\phi, \quad \phi = u,v,(a(\sigma)T + b(\sigma)\theta)$$

Applying this operator as it stands leads to an instability in high latitudes. For details of the modifications see Gadd (1983).

Table 1

List of integrations

λ =	400K	100K	25K	$K = 6.25 \times 10^{13}\ m^3\ (m^4 s^{-1} K^{-1})$
Resolution:				
Coarse	C400	C100		
Medium		M100	M25	

The relevant differences in the four integrations and their names are tabulated above. It should be noted that integrations with 50K with the coarse resolution model and 12.5K with the medium resolution both went unstable in less than ten days of integration. This sets a lower bound on the amount of diffusion needed at each resolution.

a) The effect of varying the diffusion constant

We begin by considering the effect of varying the diffusion constant at a given resolution. Figure 1 shows the zonal mean PMSL for the mean of days 31-60 of C100 and C400; for purposes of comparison Schutz and Gates (1971) January climatology and January FGGE data are also shown. In low latitudes there is not much to choose between them; in high latitudes C100 is closer to the climatologies although the difference between them is probably within the noise level of the model integrations. Figure 2 shows the PMSL fields for the mean of days 31-60 of C100 and C400. Schutz and Gates climatology of January PMSL is shown in figure 3. Both give a poor representation of the sub-Antarctic depression belt - as seen in the zonal mean. The southern subtropical highs are reasonably represented in terms of position, albeit a little weak, in both simulations. Neither simulation reproduces the climatological Azores high or the Siberian anticyclone faithfully. Both integrations produce some ridging over the Rockies although in both cases the ridging is too weak. Both have too deep Icelandic and Aleutian lows - as judged by the shaded area of less than 1000 mb. C400 positions the Aleutian low closer to the climatology than

C100. The flow over the UK is closer to the climatology in C400, there being too much of a southerly component in the flow in C100 here. In summary:on the basis of the simulated PMSL C100 and C400 suffer from similar faults and there is not much to choose between the two.

Figures 4 and 5 show the zonal mean westerly wind height-latitude cross sections for C100 and C400 and by way of comparison January FGGE data and the data of Newell et al (1972). The surface mid-latitude flow in C100 is closer to the FGGE data than in C400 as are the mid-tropospheric jets in both hemispheres. Both integrations produce excessive westerly flow at low latitudes near 300 mb compared to FGGE. Note that in the data of Newell et al there are actually easterlies here; given the much higher data coverage in FGGE in the tropics it is probable that FGGE is a better representation of reality here. C100 is marginally superior in respect of the zonal mean westerlies but both suffer from similar faults.

Table 2 Hemispheric Kinetic Energies J Kg^{-1}

		N.H.			S.H.		
Experiment		K_Z	K_S	K_T	K_Z	K_S	K_T
C100		146	41	39	53	12	21
C400		153	33	23	53	8	17
M25		130	58	48	66	14	19
M100		134	39	34	58	13	12
FGGE Jan:	EC3B	102	26	73	58	12	50
	MO3A	97	26	71	54	12	35

EC3B = ECMWF 3B analysis MO3A = UK Met Office 3A analysis.

A reasonably objective measure of model performance is the kinetic energy statistics. The hemispheric means of zonal, standing eddy and transient eddy energy for the integrations under consideration together with those from two FGGE analyses are shown in Table 2 above. (Terminology is as in Rowntree and Mitchell (1982)). Note that in both hemispheres

C100, the integration with the less diffusion, has more realistic eddy kinetic energy although in the northern hemisphere C100 does not partition the eddy kinetic energy correctly. Both integrations have too much zonal kinetic energy in the N.H., C400 being worse in this respect.

We conclude that the two integrations at the coarse resolution are of comparable quality, with C100 being marginally superior. Thus C100 will be used when comparing with the medium resolution model.

For the medium resolution model the effect of increasing the diffusion fourfold is more apparent and the choice of the smaller value a more clear cut decision. Again we start by considering the zonally averaged PMSL for the mean of the last 30 days of the 60 day integrations, M25 and M100 (figure 6). M25, the integration with the smaller diffusion constant, comes closer to the climatologies than M100 everywhere. Both deviate enormously from the climatologies in northern mid-latitudes (the 'westerly flow' problem) M100 being significantly the worse. Conversely neither integration produces a deep enough Antarctic trough and again M100 is further from climatology. M25 also reproduces the subtropical highs better than M100. The global PMSL fields (figure 7) reinforce the statement that M25 gives a superior simulation - particularly in the southern hemisphere. In the northern hemisphere both simulations suffer from similar faults: no significant ridging over the Rockies, mispositioning of the Azores and Siberian anticyclones and excessive surface westerly flow. With the possible exception of the first of these M100 emphasizes these faults more than M25.

Figure 8a shows the zonal mean westerly wind height-latitude cross sections. Again we compare them with FGGE data (Figure 5). These re-emphasize that the surface westerlies in northern mid-latitudes are excessive and that the southern mid-latitude surface flow is underestimated. M25 reproduces the mid-tropospheric jets well when contrasted with FGGE; in contrast M100 fails to close off the northern mid-tropospheric jet and has excessive westerly flow in the stratosphere around 65°N. This is consistent with the thermal structure (figs 8b and 8c) in which the north-south stratospheric temperature gradient is far too strong

in M100 in northern high latitudes. Since the two integrations have the same thermal forcing it must be the increased diffusion which causes these differences. Since the temperature gradients are as strong in M100 as they are in M25 it is probably the excessive diffusion of momentum rather than temperature which is responsible for these differences.

Comparing the kinetic energies we note that decreasing the diffusion results in a significant improvement in transient eddy energy in both hemispheres. On the other hand there is also an unrealistic increase in the standing eddy energy in the NH when the diffusion is decreased.

Although the kinetic energy statistics are inconclusive in coming to a decision on which is better, on the basis of the other information shown, the integration with the smaller diffusion constant (M25) gives the better simulated climatology.

Accordingly when assessing the effect of model resolution on the simulation we will concentrate on the integrations with the smaller amount of diffusion, i.e. M25 and C100. At the end of this section we will briefly consider M100 again, as this has the same diffusion constant as C100, and will compare them to separate out the effect of diffusion and resolution.

b) the effect of resolution

For the zonal mean PMSL (see figures 1 and 6) M25 gives a superior representation in the southern hemisphere and in the tropics; in northern mid latitudes, however, it is significantly inferior. The superiority of the PMSL field (figures 2 and 7) for M25 is clear in the southern hemisphere with a better representation of all the main features. In the northern hemisphere neither resolution gives a good representation of the Azores high or Siberian anticyclone. Aside from these faults C100, somewhat surprisingly, produces the better northern hemisphere pressure pattern, notably more realistic (i.e. less deep) Aleutian and Icelandic lows and some evidence of ridging over the Rockies.

The u cross sections also show the medium resolution simulation to be superior in the southern hemisphere and intercor in the northern hemisphere (figures 4, 5 and 8). In the southern hemisphere M25 gives a much better representation of both the surface flow and the mid-tropospheric jet - in both shape and strength - than C100, when compared to the FGGE data. M25 also simulates the tropical flow better than C100. However as indicated by the PMSL fields, the surface flow in northern mid-latitudes in M25 is far too strong; C100 is better in this respect.

Somewhat surprisingly when comparing the kinetic energies (table 2) we notice that the N.H. K_Z is stronger in C100 than in M25, despite the excessive mid-latitude westerly flow in M25. This is accounted for by the excessive westerly flow around 300 mb in the tropics in C100. In the southern hemisphere there is not much to choose between the two resolutions in terms of the kinetic energies. In the northern hemisphere M25 produces more realistic transient eddy energy but less realistic standing eddy energy.

To summarize: the medium resolution model produces a superior simulation in the tropics and in the southern hemisphere; however in the northern hemisphere some aspects of the flow are definitely better in the coarse resolution model. Why should this be? One would expect that increasing the resolution would produce an overall improvement. A possible explanation is that an important element in the momentum budget is missing. Two aspects of this have been investigated outside this study, both relating to the representation of orography, namely the use of so-called envelope orography (Wallace, Tibaldi and Simmons 1983) and the representation of gravity wave drag (Shutts and Palmer 1984). Swinbank (personal communication) has rerun M25 and C100 (renamed SGM1 and SGM2) with extra diagnostics. The zonal mean eddy momentum flux from these two integrations is compared to January 1984 mean data from the Meteorological Office operational analyses (figures 9 and 10). The northern hemisphere maximum in the coarse resolution model is about half the value in the real data but a reasonable value is achieved in the medium resolution model; note that although the total eddy momentum flux is reasonable the partition between standing and transient eddies is wrong. This is consistent with

the kinetic energy statistics for M25. A suggested explanation, then, is that whilst the medium resolution model has about the right amount of northward eddy momentum transport, because of the lack of any representation of gravity wave drag - or other orographically induced drag - the westerly winds in mid latitudes are too strong. The coarse resolution model compensates for this error by not transporting enough westerly momentum northwards and, as a result, has a more reasonable representation of the flow in the northern hemisphere. On the other hand in the southern hemisphere, where orographic effects are less important, the medium resolution model represents the momentum transport well and produces a reasonable representation of the flow field. The coarse resolution model underestimates the momentum transports and consequently underestimates the zonal mean westerly wind. To complete the explanation we observe that in mid latitudes low pressure systems play an important role in transporting momentum in the atmosphere. As Merilees' (1975) theoretical study suggests, the coarse resolution model cannot resolve (see below for more discussion on this) the scales of motion involved in the baroclinic instability process and therefore underestimates the momentum transport.

Thus while in some aspects the coarse resolution model gives a better simulation in the northern hemisphere we may speculate that, with an adequate representation of gravity wave drag, increasing the resolution will produce an unqualified improvement in the simulation when the resolution is increased.

As mentioned in the introduction Williamson (1978), supported by Merilees' (1975) theoretical study, attributes the increase in eddy activity, when the resolution is refined, to the change in lateral eddy viscosity. Indeed similar trends in both K_S and K_T are seen (table 2) when comparing M25 and M100 (increasing diffusion only) as when comparing M25 and C100 (increasing diffusion and increasing resolution). However other aspects of the integrations suggest that the change in resolution has as much effect as changing the diffusion. Examination of the PMSL fields for M25, M100 and C100 (figures 2 and 7) suggest that, although in the southern hemisphere M100 'lies between' M25 and C100, in the northern mid latitudes

M100 has more extreme westerly flow over Asia than either M25 or C100. In terms of the u height-latitude cross sections M100 is much more similar to M25 than to C100. Therefore we conclude that changing resolution has as much effect on the simulation as changing the diffusion.

A similar study has been conducted by MHH using the GFDL spectral model at three different resolutions. We reproduce two figures from their paper. Figure 11 shows zonal mean PMSL from the three spectral resolutions and the fields are shown in figure 12. Note that spectral truncations M30 and M15 correspond approximately to the medium and coarse resolution models respectively. As in the Meteorological Office grid point model the effect of increasing the resolution is to deepen the depression belts in both hemispheres and to increase the intensity of the subtropical highs. The M30 integration suffers from faults similar to those in the medium resolution model particularly in the northern hemisphere; specifically the excessively deep climatological lows, the misplaced Azores and Siberian highs, lack of ridging over the Rockies and excessive westerly flow. This reinforces the conclusion that the faults in the simulation are due to a failure to represent some physical mechanism rather than a fault in the numerical technique - the spectral dynamics being so different to the finite difference dynamics.

3. The July Integrations

For this season we concentrate on the effect of resolution. In passing we note that integrations with various values of the diffusion constant were run for the coarse resolution model with perpetual July forcing conditions, and again the value 100K ($K = 6.25 \times 10^{13}$ m^3) gave the best simulation. Only one value of the diffusion constant, 25K, was used in the medium resolution model. Both integrations started from the same initial data (derived from FGGE data of 10/6/79) and had radiation conditions, sea surface temperatures and sea-ice extents fixed for July. The physical parametrizations were the same as those in the January integrations. The medium resolution integration is named MJ25 and the coarse resolution CJ100. The means of days 31-60 are used for the comparison.

First we consider the zonal mean PMSL of the two integrations (figure 13). Apart from the southern sub tropical highs the medium resolution model is superior everywhere. In particular note the improvement in the southern depression belt and the northern hemisphere highs - very poorly treated by CJ100 - as the resolution increases. The coarse resolution model produces a very unrealistic pressure pattern (figure 14) particularly in the northern hemisphere where the circulation is dominated by the continental heat lows and oceanic anticyclones; this is particularly apparent with the Asian monsoon which is much too intense when contrasted with Schutz and Gates (1972) climatology (figure 15). Other poor features in CJ100 are a spurious high pressure belt to the north of the Eurasian continent and a failure to reproduce the northern subtropical highs. In contrast the southern subtropical highs are reproduced well but, as we saw in the zonal mean, the sub-Antarctic depression belt is not deep enough. Nearly all these faults decrease when the resolution increases. In MJ25 the monsoon heat low is more realistic, there is a reasonable simulation of the Azores and Pacific highs and the high latitude pressure field is more realistic in both hemispheres. The only detrimental features are the southern subtropical highs. To summarize: there is an overall significant improvement in the pressure field when the resolution is increased.

We next compare the zonal mean westerly wind cross sections with July FGGE data and the June - August mean data of Newell et al (1972) (figures 16 and 17). MJ25 gives a better overall representation, notably the strength and structure of the mid-tropospheric jets, the overall u field in the tropics and the southern mid-latitude surface flow. One fault in the medium resolution simulation is excessive high tropospheric easterlies in the tropics.

Table 3 Hemispheric Kinetic Energies: July Integrations J Kg^{-1}

	N.H.			S.H.		
Experiment	K_Z	K_S	K_T	K_Z	K_S	K_T
CJ100	29	24	12	154	28	39
MJ25	45	19	12	171	23	50
FGGE EC3B	22	13	33	128	13	64
M03A	22	14	37	127	14	52

Next we contrast the hemispheric kinetic energy statistics. The K_Z from MJ25 is excessive in both hemispheres mainly because of the aforementioned excessive tropical easterlies; CJ100 is superior in this respect. There is an improvement in both standing and transient eddy energies when the resolution is increased. However the transient eddy kinetic energy in the northern hemisphere remains grossly deficient.

Finally we reproduce the July PMSL zonal mean and fields for the three spectral resolutions studied by MHH (Figures 18 and 19). Very similar trends are observed. The excessive continental heat lows and the spurious high pressure belt north of the Eurasian continent are faults common to the M15 July integration and the coarse resolution integration. The main fault in the medium resolution model - the excessively intense southern subtropical highs - also occurs in the M30 integration.

4. Conclusion and Summary

In the July integrations there is an overall improvement in the simulation as the resolution is increased. This is not the case for the northern winter simulation. However there is some evidence that the coarse resolution model's apparently superior northern winter simulation is due to a cancellation of errors. We may hope that with the correction of one of these errors - perhaps by the introduction of a parametrized gravity wave drag - there will be an overall improvement as the resolution increases.

In agreement with Williamson it was found that the increase in eddy activity associated with the higher resolution integrations may be attributed to the decrease in diffusion. However, other aspects of the circulation - for example the mid-latitude surface westerly flow in the northern winter experiments - are affected more by the change in resolution than by the change in diffusion constant.

References

Clarke, R.H. 1970 Recommended methods for the treatment of the boundary layer in numerical models. Austr. Met. Mag., 18, 51-73.

Crutcher, H.L. 1970 Selected level heights, temperatures and dewpoints for the Northern Hemisphere. NAVAIR50-1C-52 US Nav Weath Serv Command, Washington DC.

Gadd, A.J. 1983 Some thoughts on diffusion, Met O 20 Internal Note No. 13.

Lyne, W.H. and Rowntree, P.R. 1976 Development of a convective parametrization using GATE data. Met O 20 Technical Note II/70.

Manabe, S., Smagorinsky, J., Holloway, L., and Stone, M.H. 1970 Simulated Climatology of a General Circulation Model with a Hydrological Cycle III Effects of increased computational resolution. MWR 98 pp 175-213.

Manabe, S., Hahn, D.G., and Holloway, J.L., 1979, Climate Simulations with GFDL Spectral Models of the Atmosphere, in GARP Publication Series No 22 Vol 1.

Merilees, P.E., 1975, The effect of grid resolution on the instability of a simple baroclinic model. M.W.R. 103 pp 101-104.

Newell, R.E., Kidson, J.W., Vincent, D.G., and Boer, G.J., 1972, The general circulation of the tropical atmosphere and interactions with extratropical latitudes. Vol. 1, MIT Press.

Rowntree, P.R., and Mitchell, J.F.B., 1982 Preliminary analyses of 50-day integrations of the Met O 20 CYBER model. Met O 20 Technical Note No. II/194.

Schutz, C., and Gates, W.L., 1971, Global climatic data for the surface, 800 mb, 400 mb: January. R-915-ARPA, Rand, Santa Monica, California.

Schutz, C., and Gates, W.L., 1972, Global climatic data for the surface, 800 mb, 400 mb: July. R-1029-ARPA, Rand, Santa Monica, California.

Shutts, G. and Palmer, T. 1984 "Preliminary results of the effect of a parametrization of gravity wave drag in the Met Office 11-layer operational model". Met O 13 Internal Note No. 149.

Taljaard J.J., van Loon H., Crutcher, H.L. and Jenne R.L. 1969 Climate of the upper air 1. Southern Hemisphere Vol 1. Temperatures, dew points and heights at selected pressure levels. NAVAIR 50-1C-55 US Nav Weath Serv, Washington DC.

Wallace, J.M., Tibaldi, S., and Simmons, A.J., 1983 Reduction of systematic forecast errors in the ECMWF model through the introduction of an envelope orography. Q.J.R.M.S. 109 pp 683-718.

Williamson, D.L., 1978, The Relative Importance of Resolution, Accuracy and Diffusion in Short Range Forecasts with the NCAR Global Circulation Model. M.W.R. 106 pp 69-88.

Figure Captions

Figure 1. Zonally averaged sea level pressure (mb): C100, C400 and January observed.

Figure 2. Sea level pressure (mb): C100, C400.

Figure 3. Observed sea level pressure (mb) for January.

Figure 4. Zonally averaged zonal wind (ms^{-1}): C100, C400.

Figure 5. " " " " " : January observed. (FGGE and Newell et al, 1972).

Figure 6. As Fig. 1: M100, M25 and observed.

Figure 7. As Fig. 2: M25, M100.

Figure 8(a) As Fig. 4: M25, M100.

Figure 8(b) Zonally averaged temperature: M100, M25.

Figure 8(c) " " " : observed.

Figure 9. Zonally averaged northward eddy momentum flux (m^2s^{-2}) at 250 mb: SGM1, SGM2.

Figure 10. As Figure 9 for January 1984 analyses.

Figure 11. Zonally averaged sea level pressure for January GFDL experiments.

Figure 12. Sea level pressure for January GFDL experiments.

Figure 13. As Figure 1: CJ100, MJ25

Figure 14. As Figure 2: CJ100, MJ25

Figure 15. Observed sea level pressure (mb) for July.

Figure 16. As Fig. 4: CJ100, MJ25.

Figure 17. As Fig. 5 for July.

Figure 18. As Fig. 11 for July.

Figure 19. As Fig. 12 for July.

Figure 1

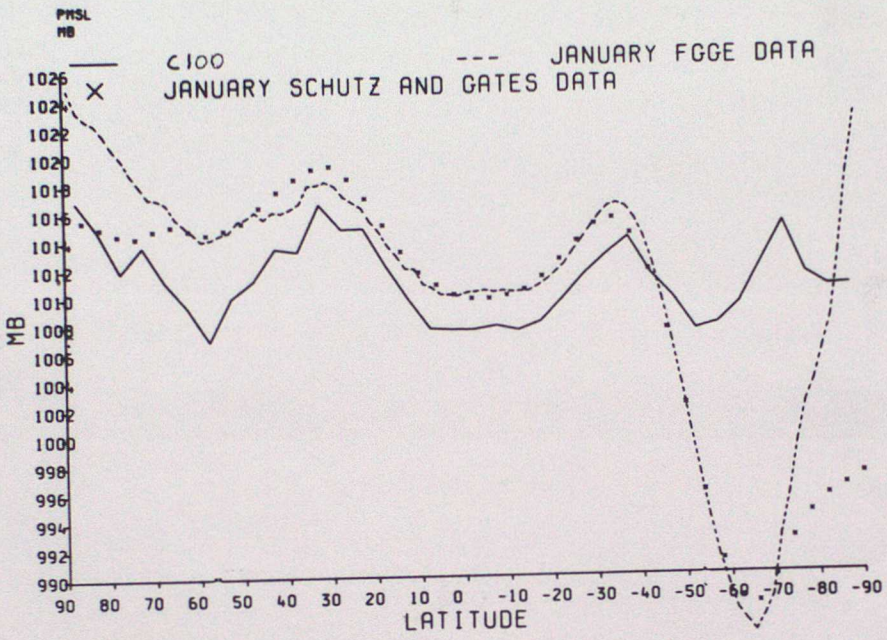
PMSL
MB
C100
JANUARY SCHUTZ AND GATES DATA
--- JANUARY FGGE DATA
MB
LATITUDE

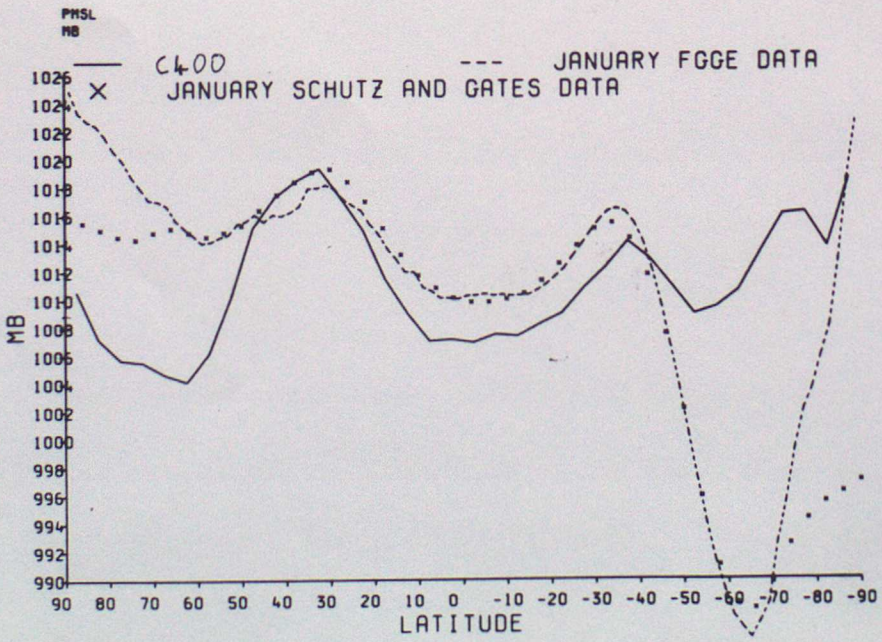
PMSL
MB
C400
JANUARY SCHUTZ AND GATES DATA
--- JANUARY FGGE DATA
MB
LATITUDE

Figure 2

C100 : COARSE RESOLUTION JANUARY INTEGRATION
WITH 100K DIFFUSION CONSTANT PMSL
AVERAGE FROM 0.15Z ON DAY 31 TO 0Z ON DAY 60
LEVEL: SEA LEVEL EXPERIMENT NO.: 1308

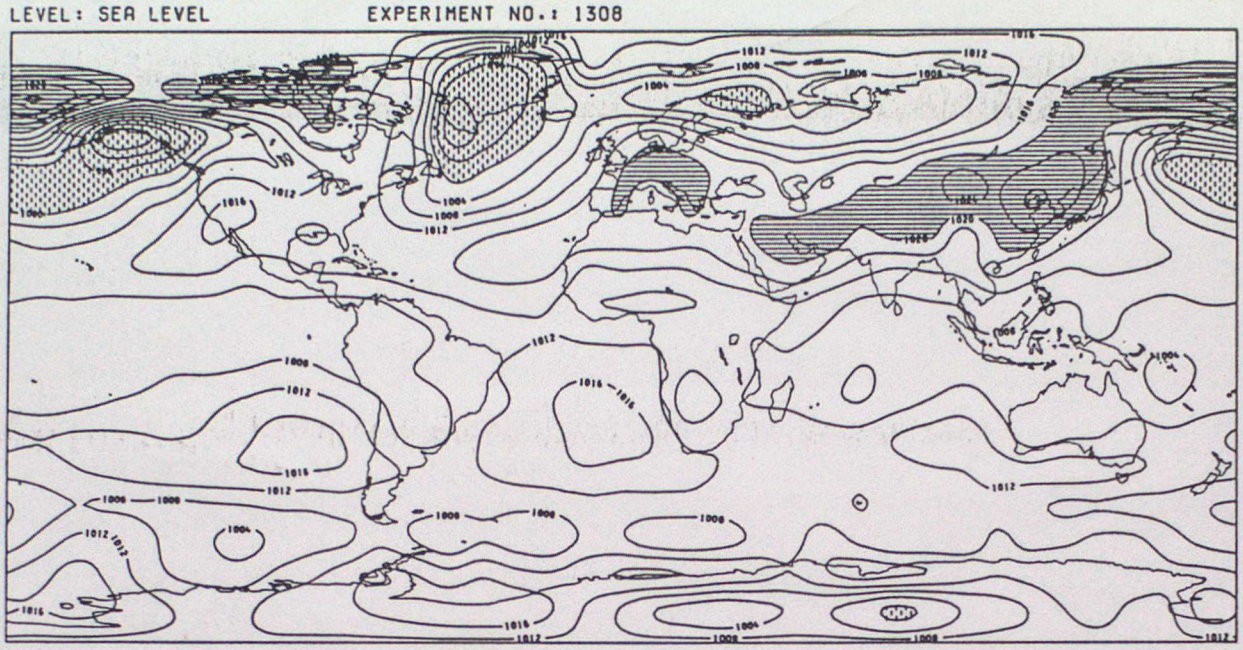

C400 : COARSE RESOLUTION JANUARY INTEGRATION
WITH 400K DIFFUSION CONSTANT PMSL
AVERAGE FROM 0.15Z ON DAY 31 TO 0Z ON DAY 60
LEVEL: SEA LEVEL EXPERIMENT NO.: 1310

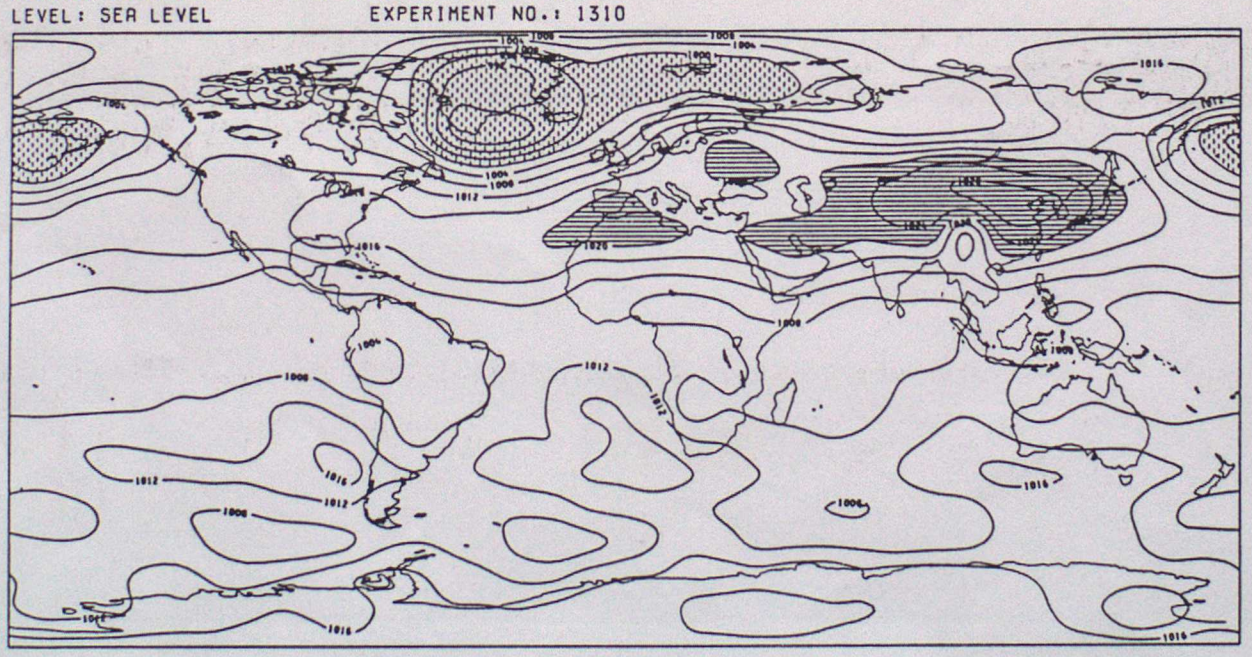

Figure 3

SCHUTZ AND GATES CLIMATOLOGICAL DATA FOR JANUARY
PMSL
AVERAGE FROM 0Z ON 1/1 DAY 1 TO 0Z ON 31/1 DAY 31
LEVEL: SEA LEVEL

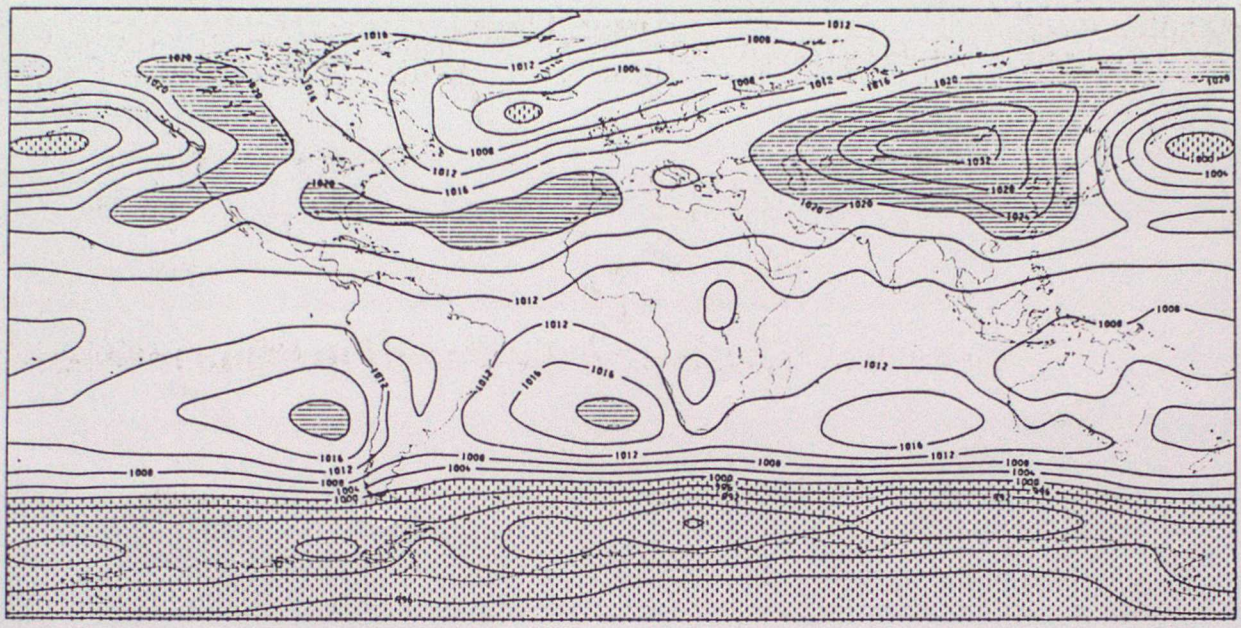

Figure 4

C100
WESTERLY WIND
AVERAGE FROM 0.15Z ON DAY 31 TO 0Z ON DAY 60
ZONAL AVERAGE EXPERIMENT NO.: 1308

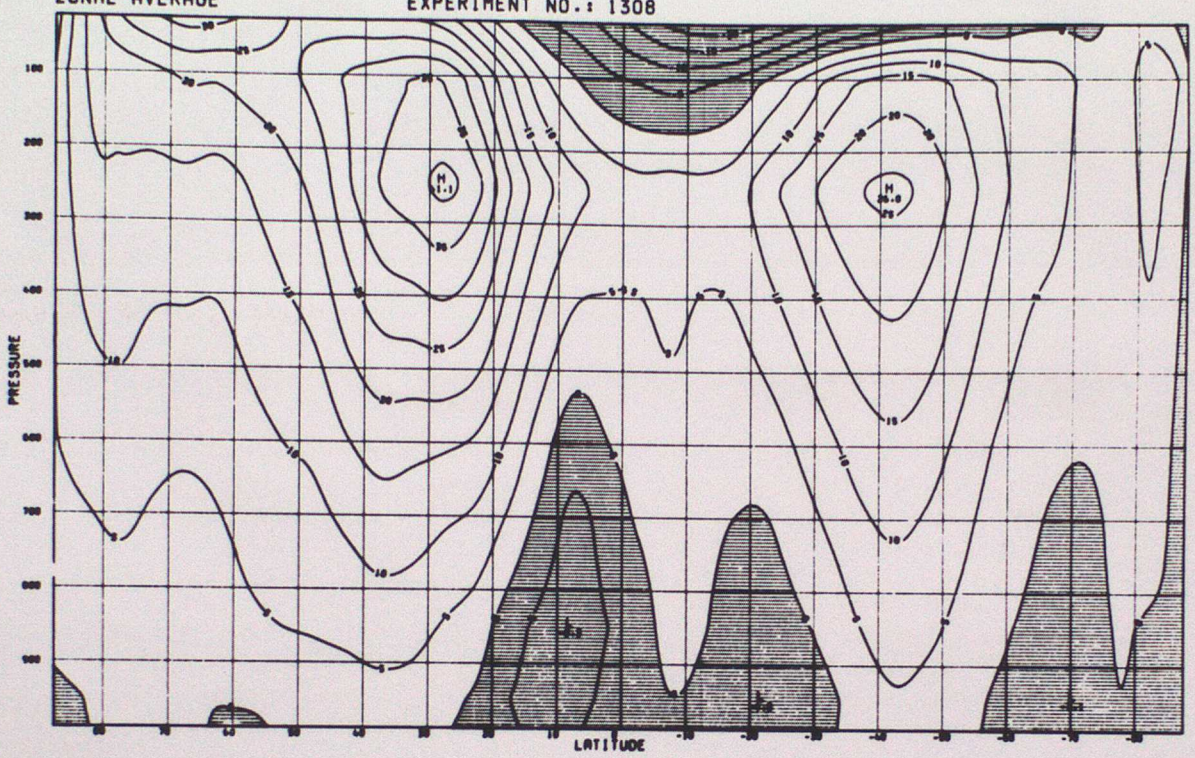

C400
WESTERLY WIND
AVERAGE FROM 0.15Z ON DAY 31 TO 0Z ON DAY 60
ZONAL AVERAGE EXPERIMENT NO.: 1310

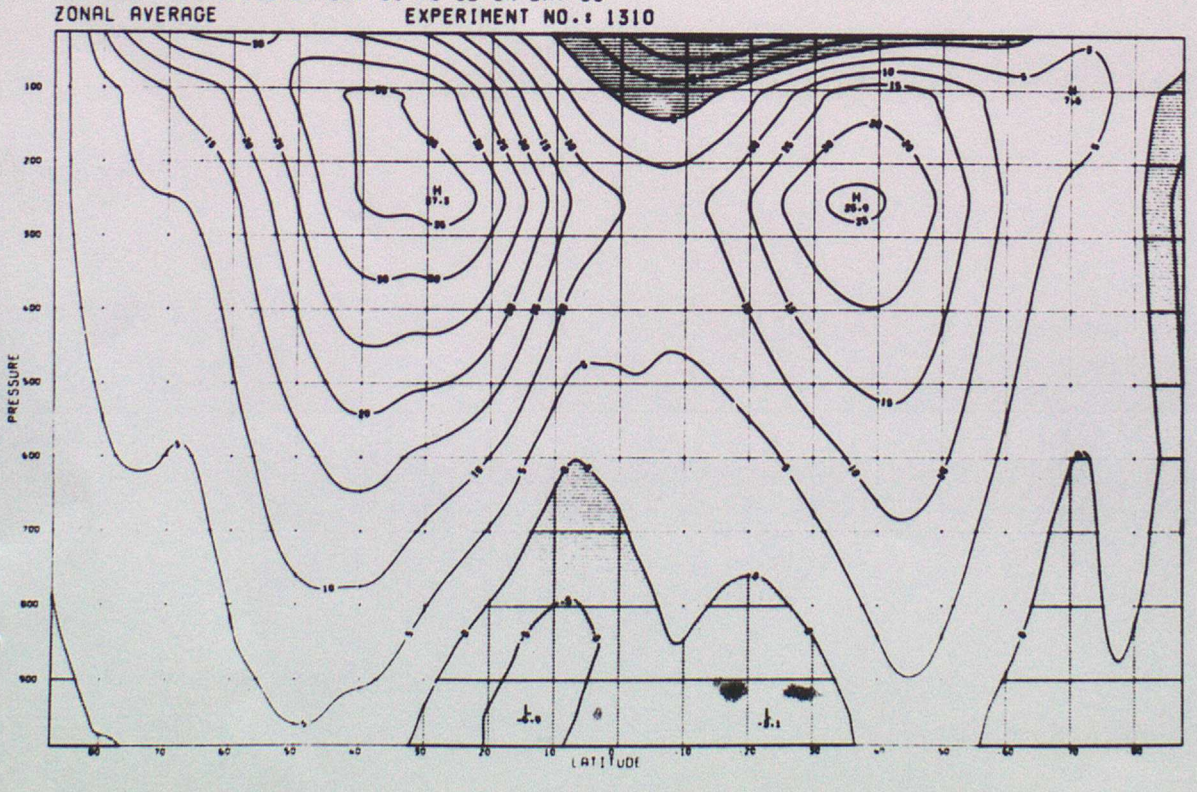

Figure 5

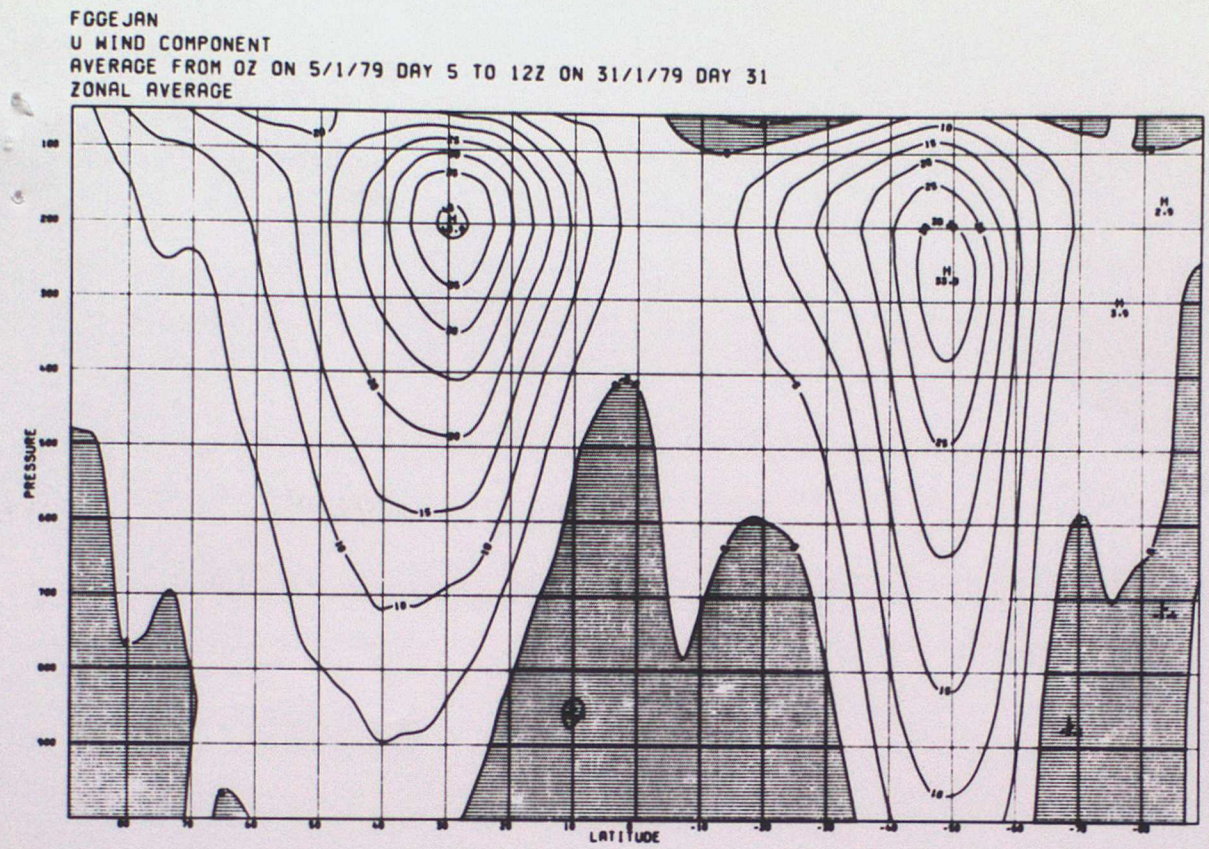
FGGEJAN
U WIND COMPONENT
AVERAGE FROM OZ ON 5/1/79 DAY 5 TO 12Z ON 31/1/79 DAY 31
ZONAL AVERAGE
PRESSURE
LATITUDE

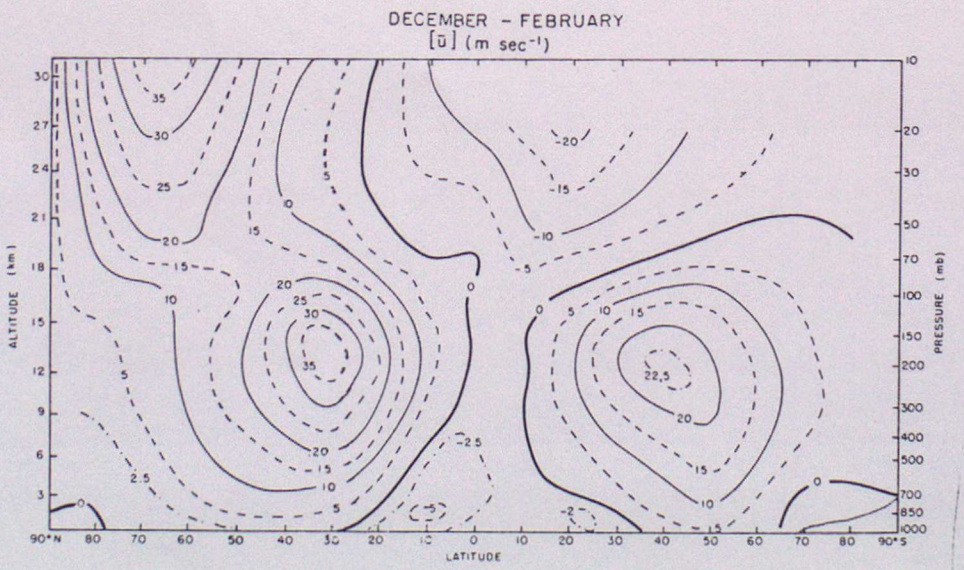
DECEMBER - FEBRUARY
[ū] (m sec⁻¹)
ALTITUDE (km)
PRESSURE (mb)
LATITUDE
90°N
90°S

Figure 6

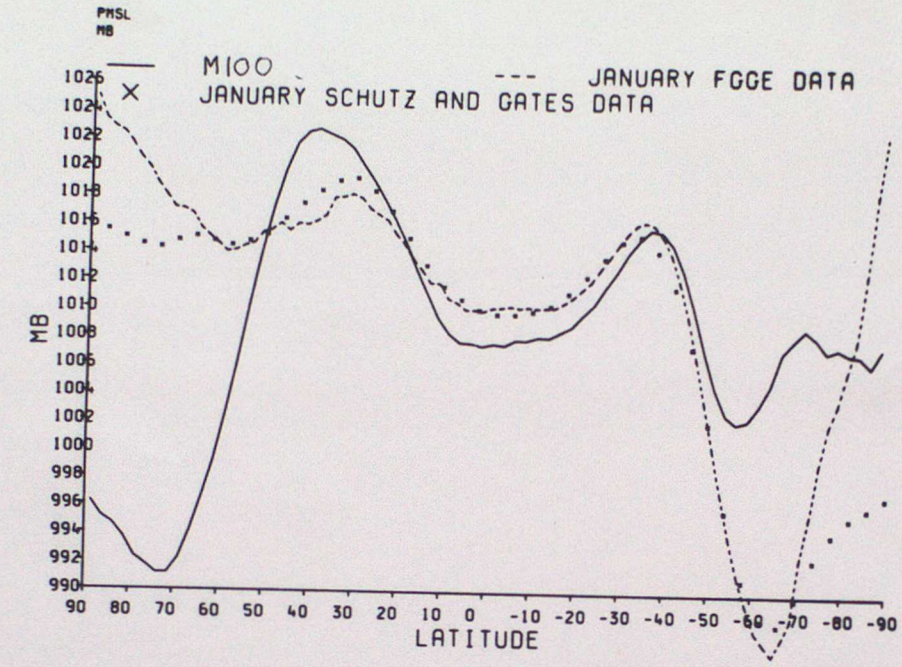
PMSL
MB
M100
JANUARY SCHUTZ AND GATES DATA
--- JANUARY FGGE DATA
MB
1026
1024
1022
1020
1018
1016
1014
1012
1010
1008
1006
1004
1002
1000
998
996
994
992
990
90 80 70 60 50 40 30 20 10 0 -10 -20 -30 -40 -50 -60 -70 -80 -90
LATITUDE

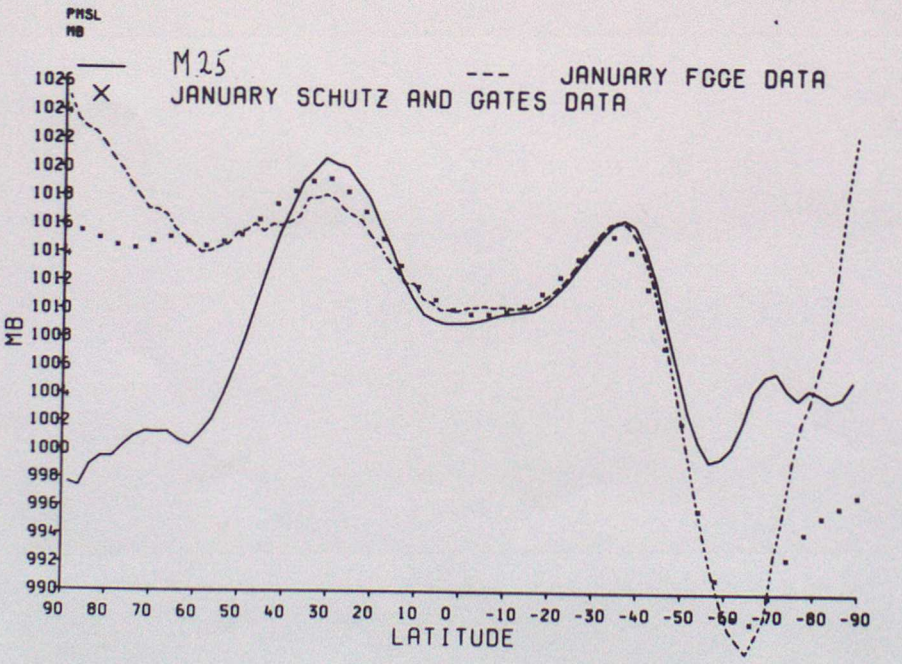
PMSL
MB
M25
JANUARY SCHUTZ AND GATES DATA
--- JANUARY FGGE DATA
MB
1026
1024
1022
1020
1018
1016
1014
1012
1010
1008
1006
1004
1002
1000
998
996
994
992
990
90 80 70 60 50 40 30 20 10 0 -10 -20 -30 -40 -50 -60 -70 -80 -90
LATITUDE

Figure 7

M 25 : MEDIUM RESOLUTION JANUARY INTEGRATION
WITH 25*K DIFFUSION CONSTANT PMSL
AVERAGE FROM 0.15Z ON DAY 31 TO 0Z ON DAY 60
LEVEL: SEA LEVEL EXPERIMENT NO.: 1243

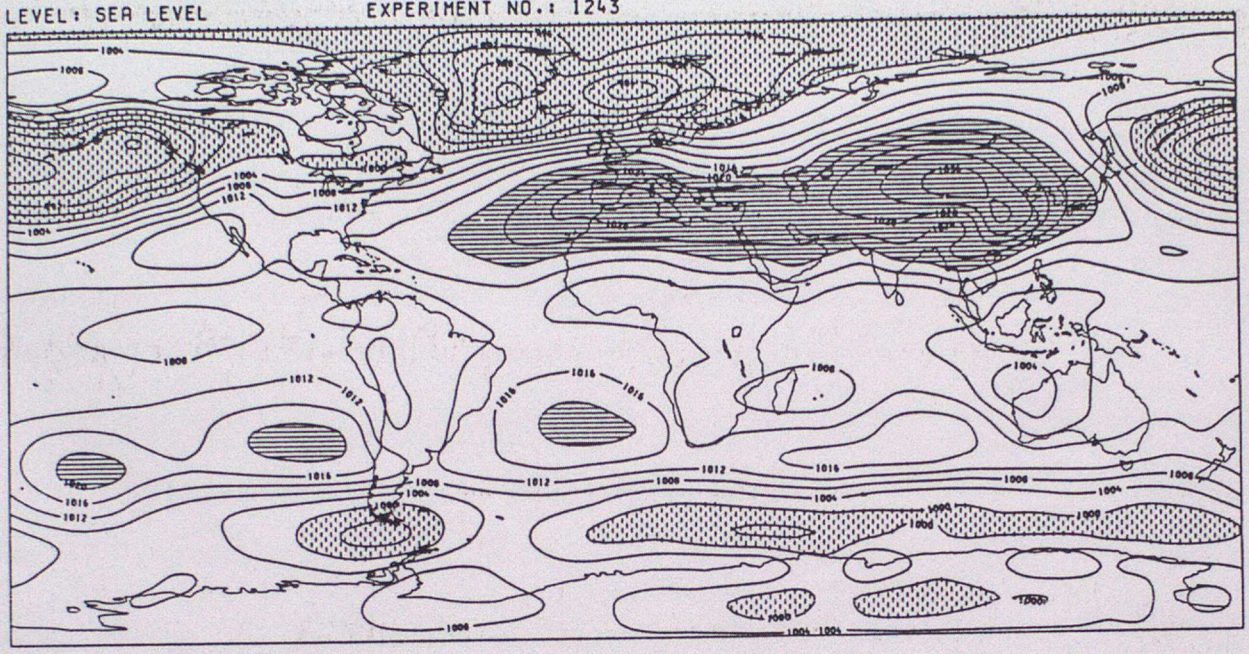

M100 : MEDIUM RESOLUTION JANUARY INTEGRATION
WITH 100*K DIFFUSION CONSTANT PMSL
AVERAGE FROM 0.15Z ON DAY 31 TO 0Z ON DAY 60
LEVEL: SEA LEVEL EXPERIMENT NO.: 1249

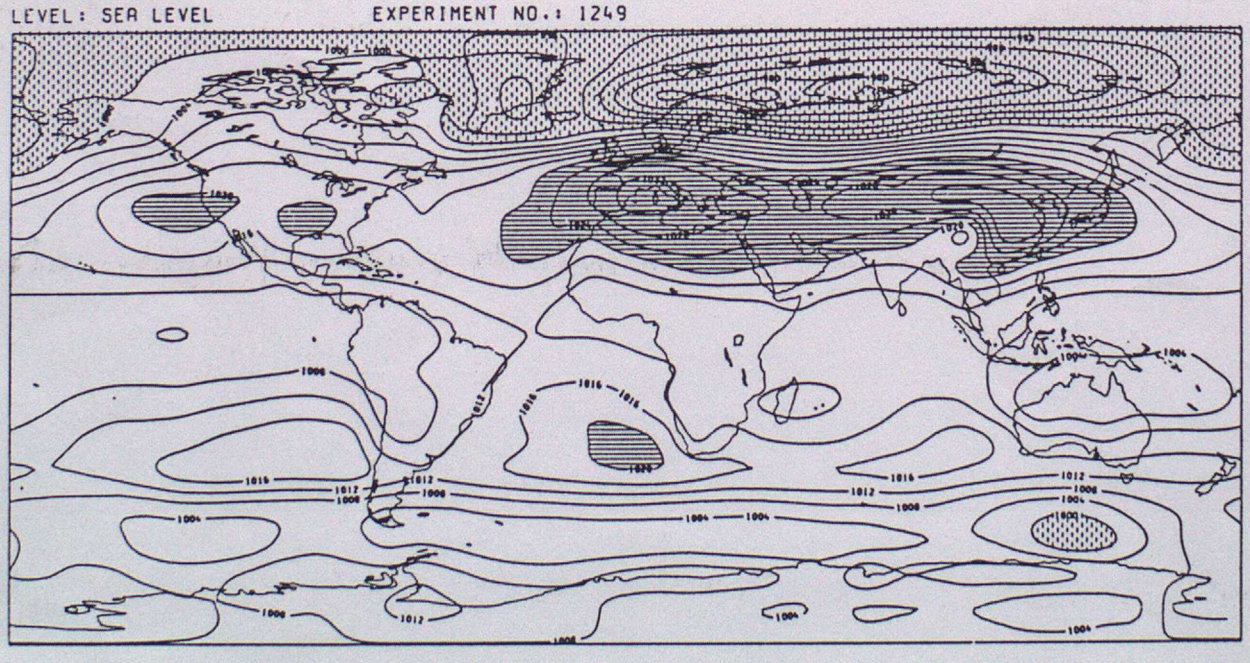

Figure 8a

M25
MEDIUM RESOLUTION JAN 25=K DIFFUSION
WESTERLY WIND
AVERAGE FROM 0.15Z ON DAY 31 TO 0Z ON DAY 60
ZONAL AVERAGE EXPERIMENT NO.: 1243

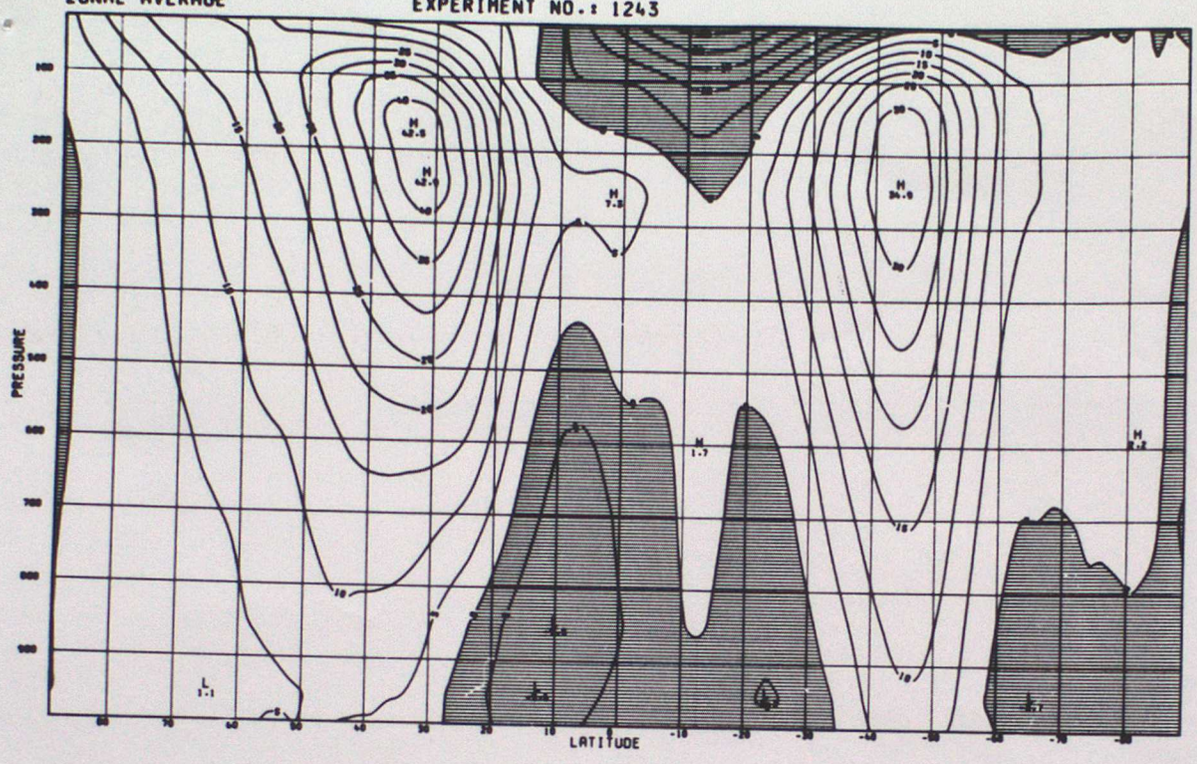

M100
MEDIUM RESOLUTION JAN 100 K DIFFUSION
WESTERLY WIND
AVERAGE FROM 0.15Z ON DAY 31 TO 0Z ON DAY 60
ZONAL AVERAGE EXPERIMENT NO.: 1249

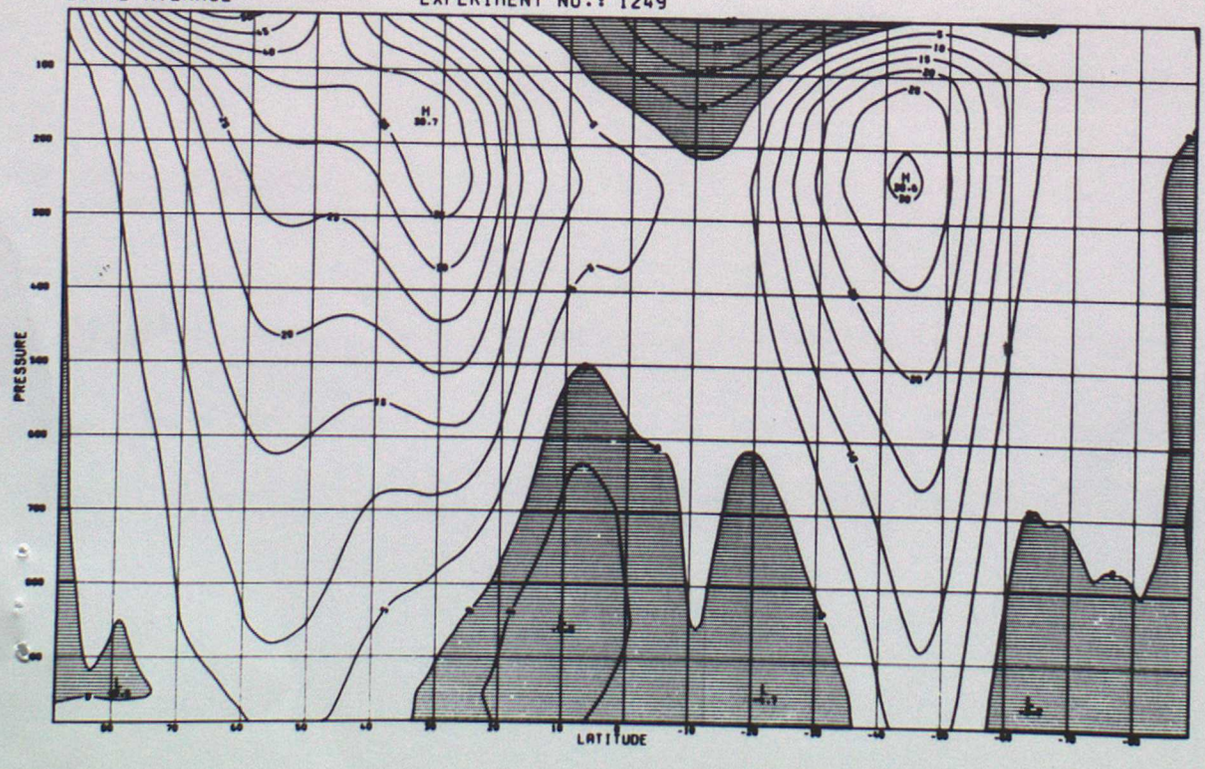

Figure 8c

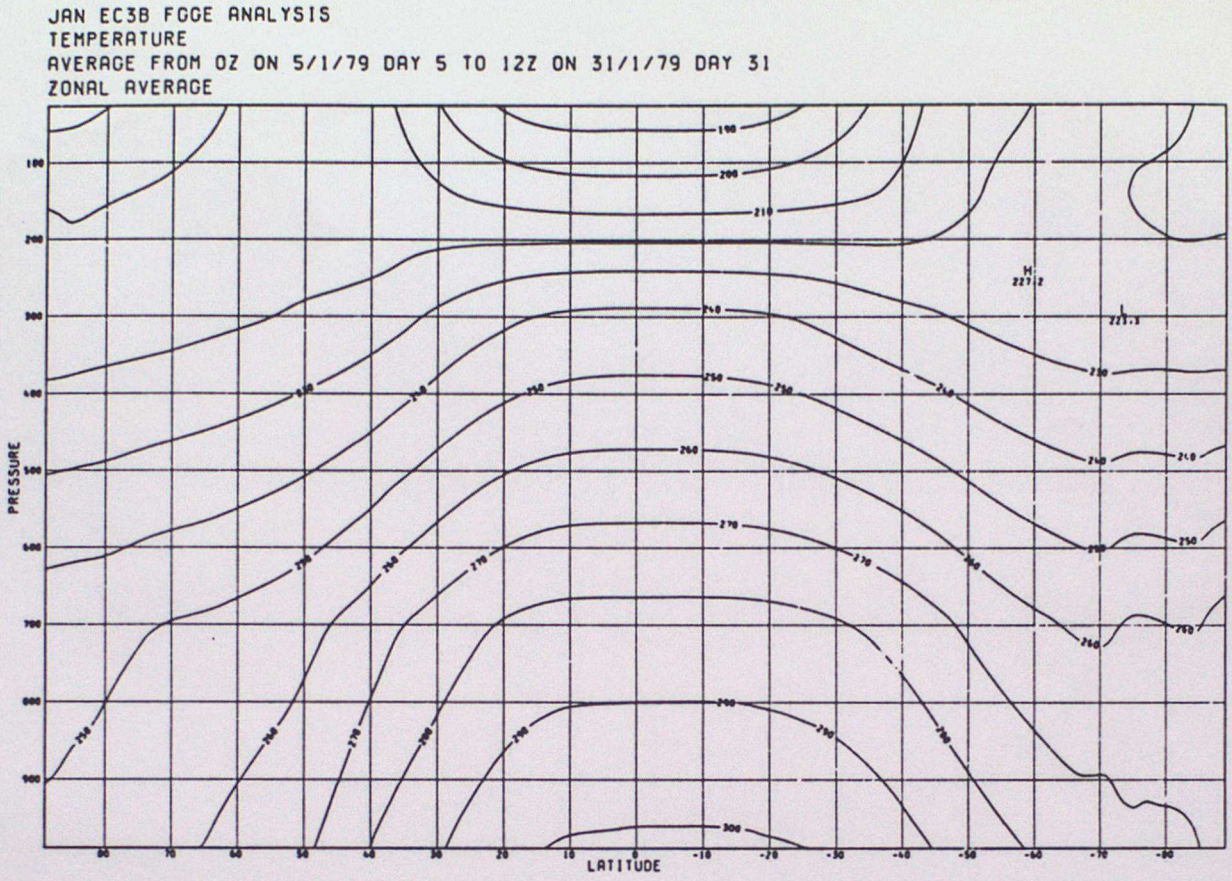
JAN EC3B FGGE ANALYSIS
TEMPERATURE
AVERAGE FROM 0Z ON 5/1/79 DAY 5 TO 12Z ON 31/1/79 DAY 31
ZONAL AVERAGE
PRESSURE
LATITUDE

Figure 9

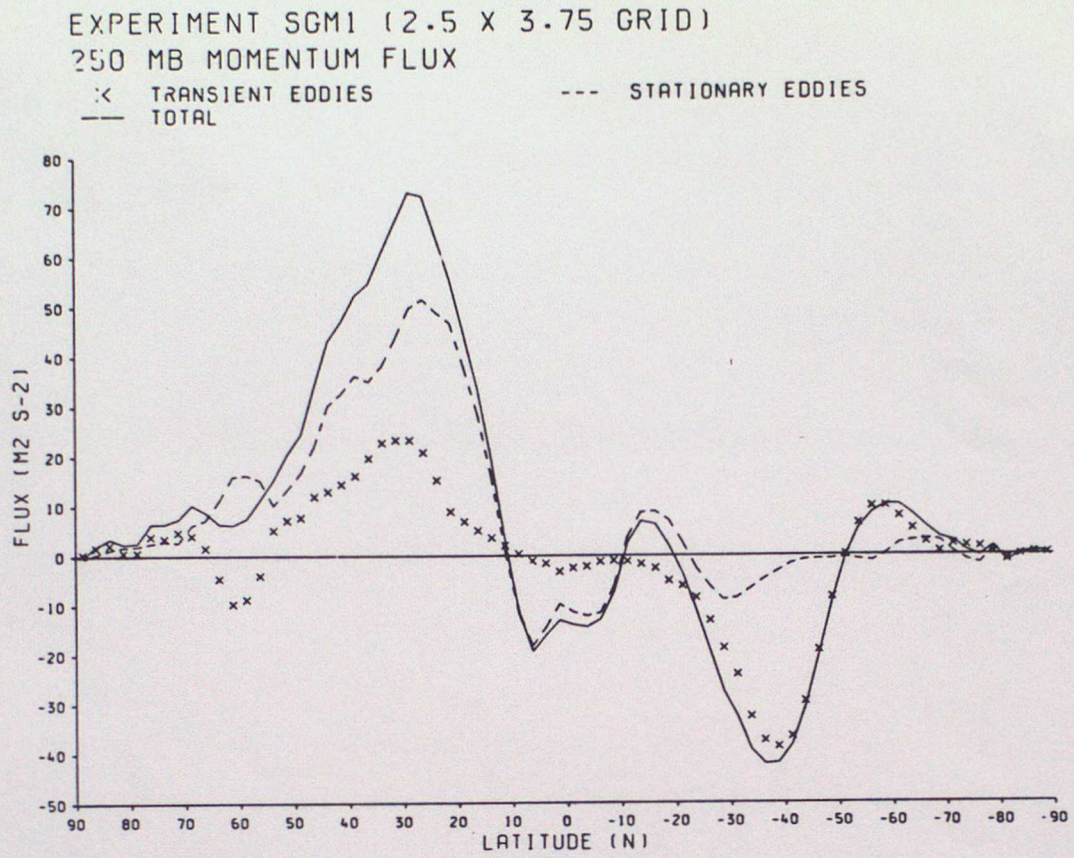
EXPERIMENT SGM1 (2.5 X 3.75 GRID)
250 MB MOMENTUM FLUX
× TRANSIENT EDDIES
--- STATIONARY EDDIES
—— TOTAL
FLUX (M2 S-2)
LATITUDE (N)

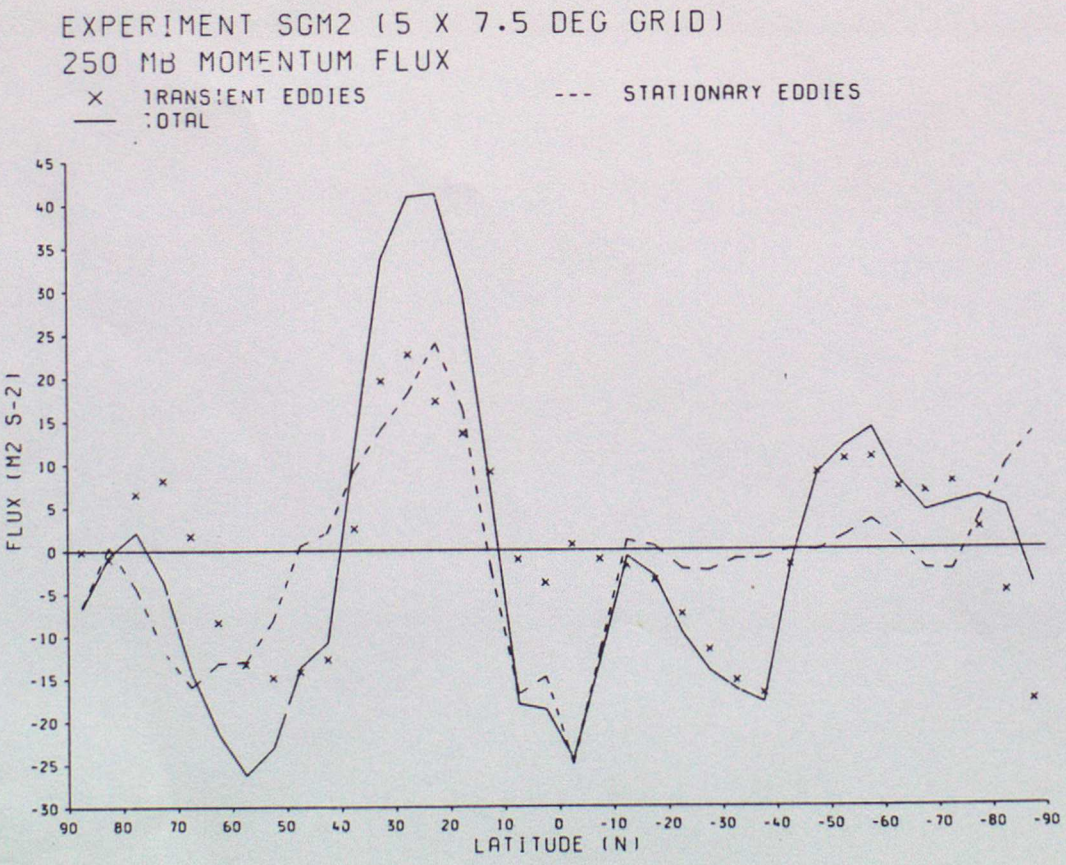
EXPERIMENT SGM2 (5 X 7.5 DEG GRID)
250 MB MOMENTUM FLUX
× TRANSIENT EDDIES
--- STATIONARY EDDIES
—— TOTAL
FLUX (M2 S-2)
LATITUDE (N)

Figure 10

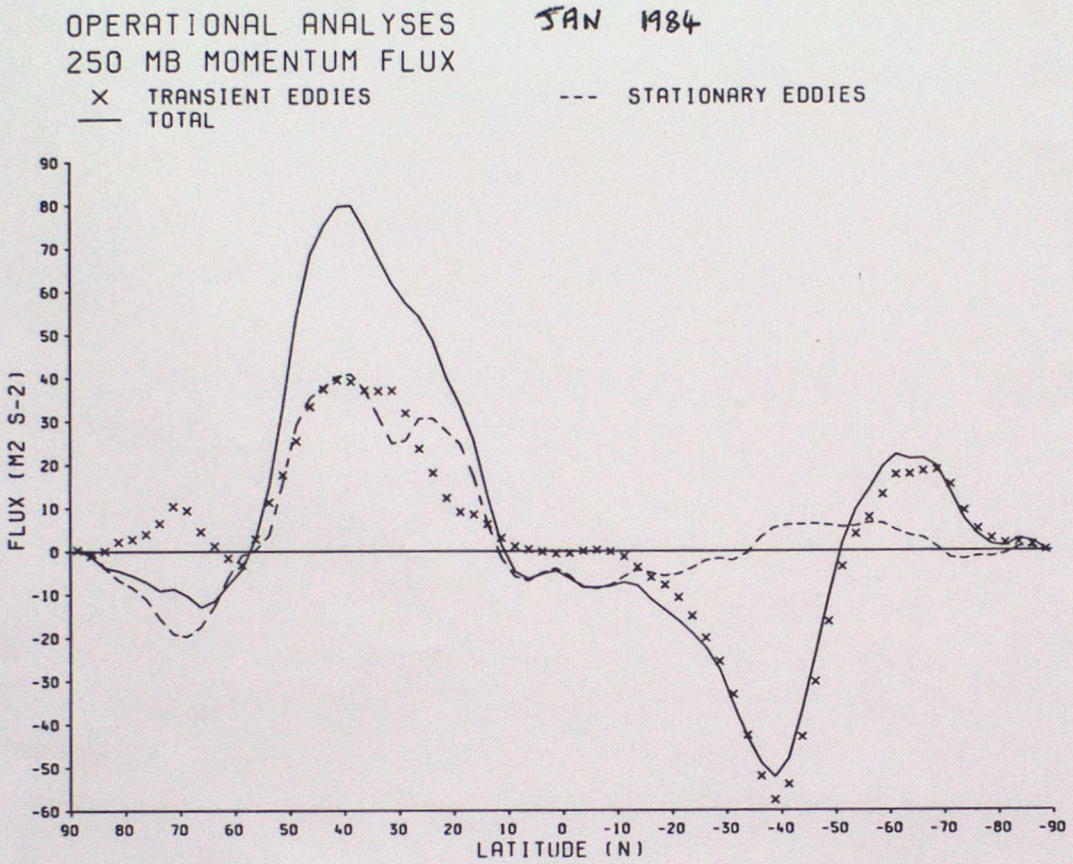
OPERATIONAL ANALYSES
JAN 1984
250 MB MOMENTUM FLUX
× TRANSIENT EDDIES
--- STATIONARY EDDIES
TOTAL
FLUX (M2 S-2)
90
80
70
60
50
40
30
20
10
0
-10
-20
-30
-40
-50
-60
90 80 70 60 50 40 30 20 10 0 -10 -20 -30 -40 -50 -60 -70 -80 -90
LATITUDE (N)

Figure 11

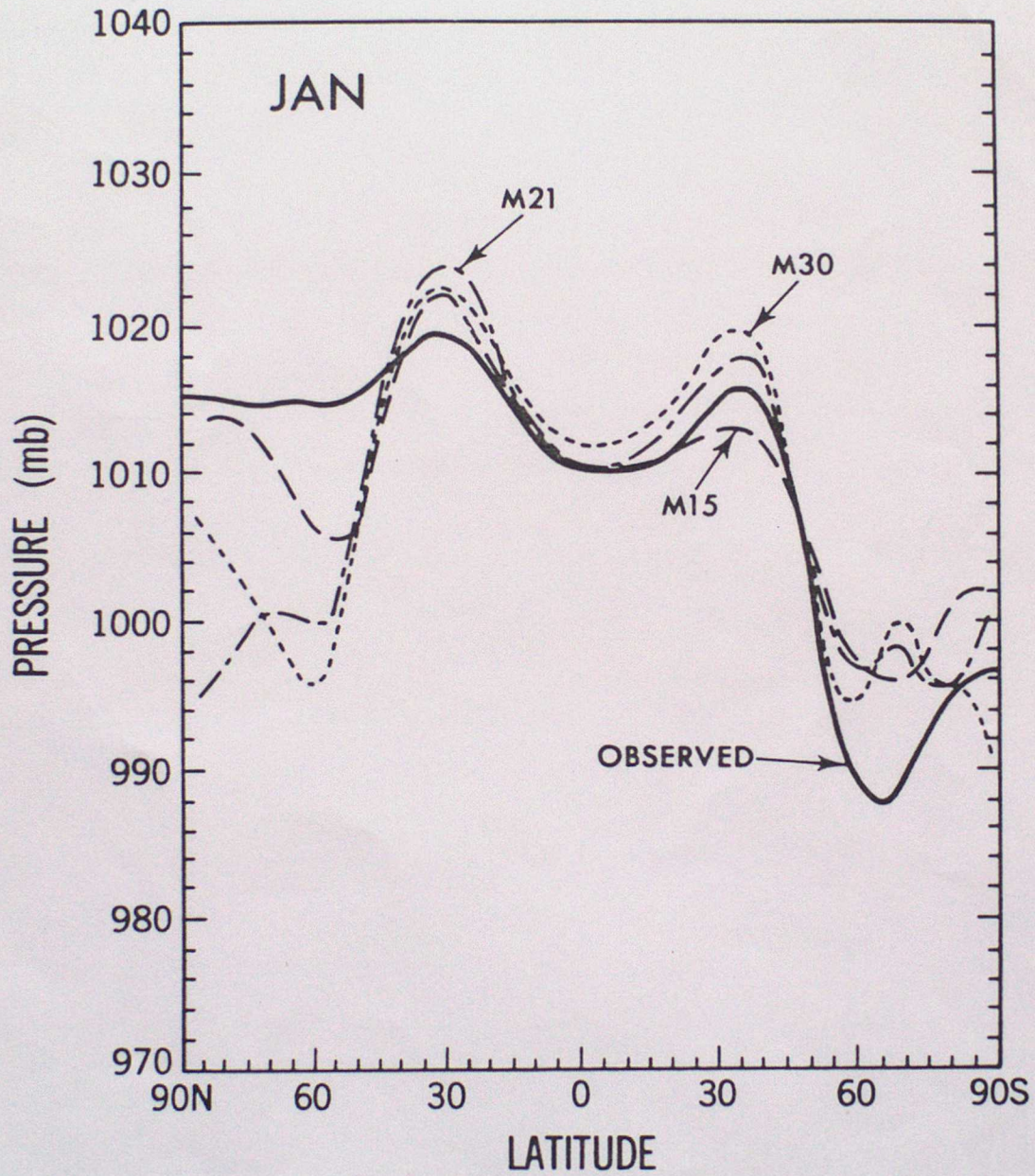

Latitudinal distributions of the January zonal mean sea level pressure (mb) for the M15, M21 and M30 spectral models and as observed (Crutcher and Meserve, 1970, and Taljaard *et al.*, 1969).

Figure 12

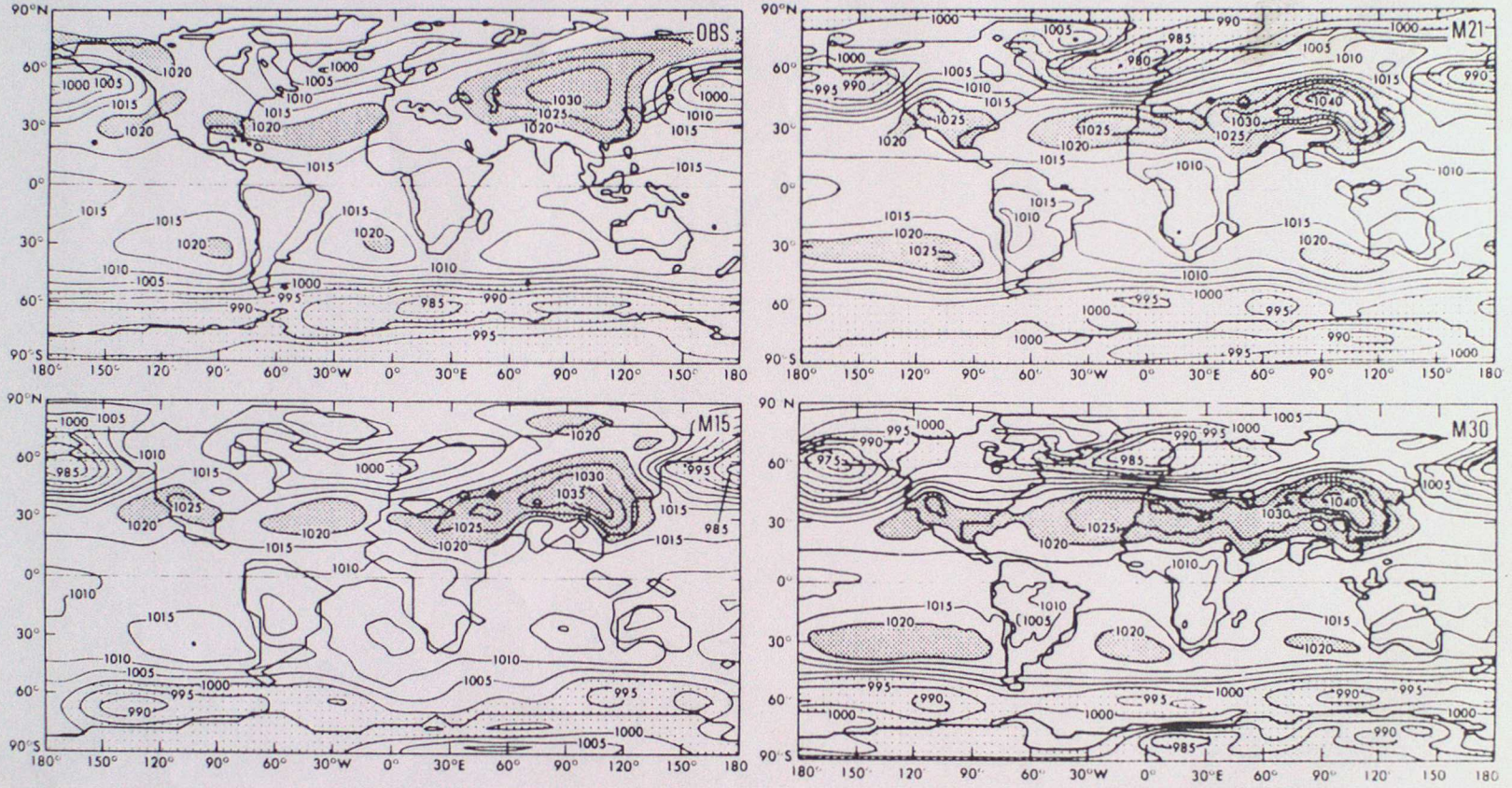

Geographical distributions of the January mean sea level pressure (mb) for the M15, M21 and M30 spectral models and observed (Crutcher and Meserve, 1970, and Taljaard *et al.*, 1969).

Figure 13

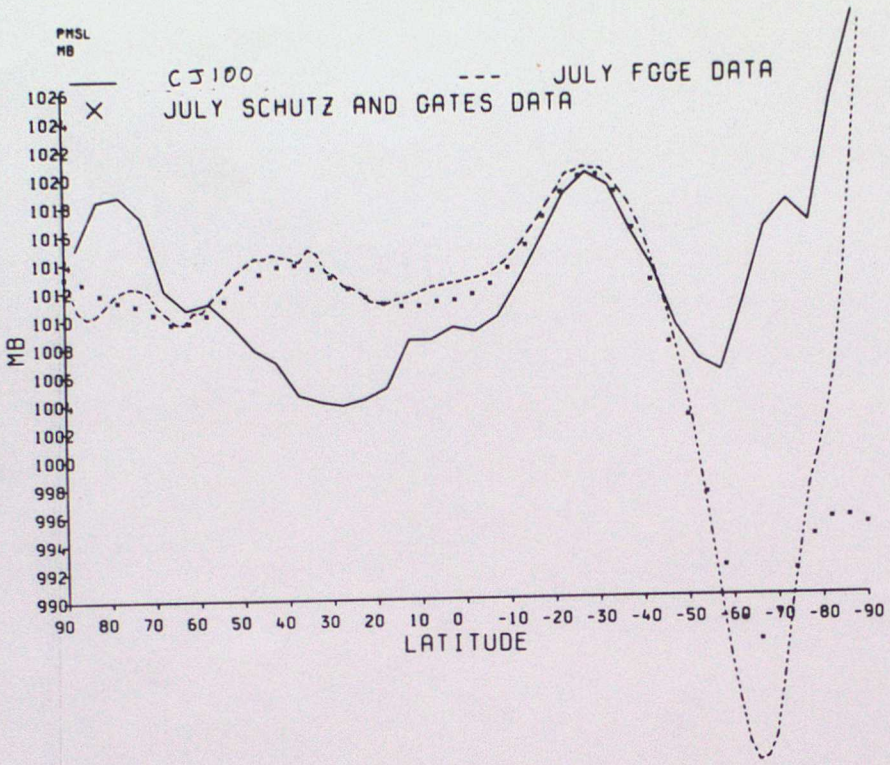
PMSL
MB
CJ100
--- JULY FGGE DATA
X JULY SCHUTZ AND GATES DATA
MB
LATITUDE

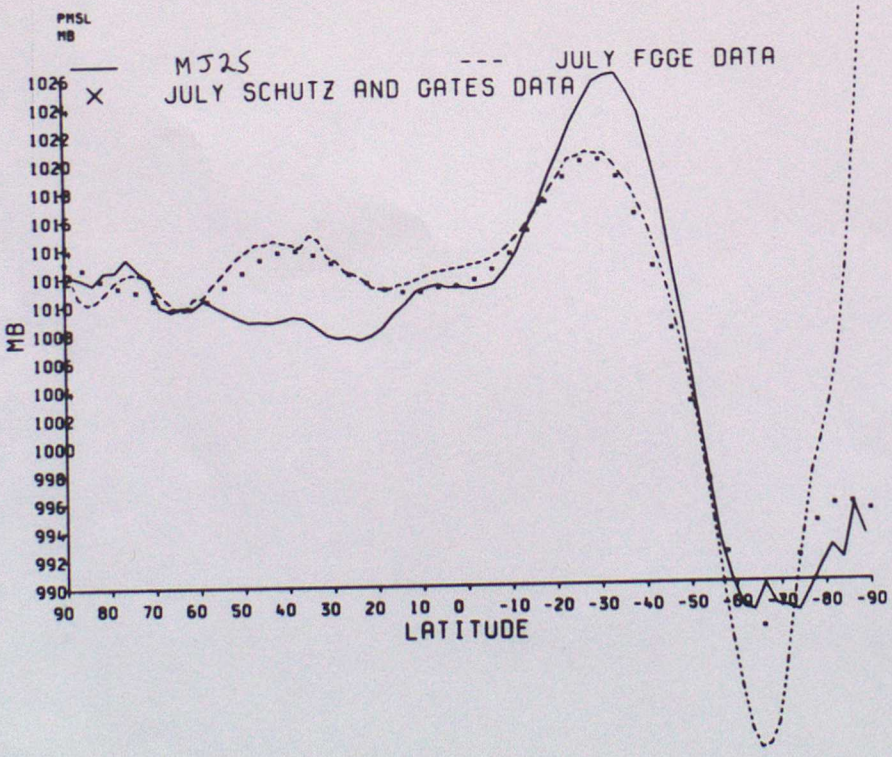
PMSL
MB
MJ25
--- JULY FGGE DATA
X JULY SCHUTZ AND GATES DATA
MB
LATITUDE

Figure 14

CJ100 : COARSE RESOLUTION JULY INTEGRATION
WITH 100 K DIFFUSION CONSTANT PMSL
AVERAGE FROM 0Z ON 2/12 DAY 31 TO 0Z ON 1/1/1 DAY 60
LEVEL: SEA LEVEL EXPERIMENT NO.: 1314

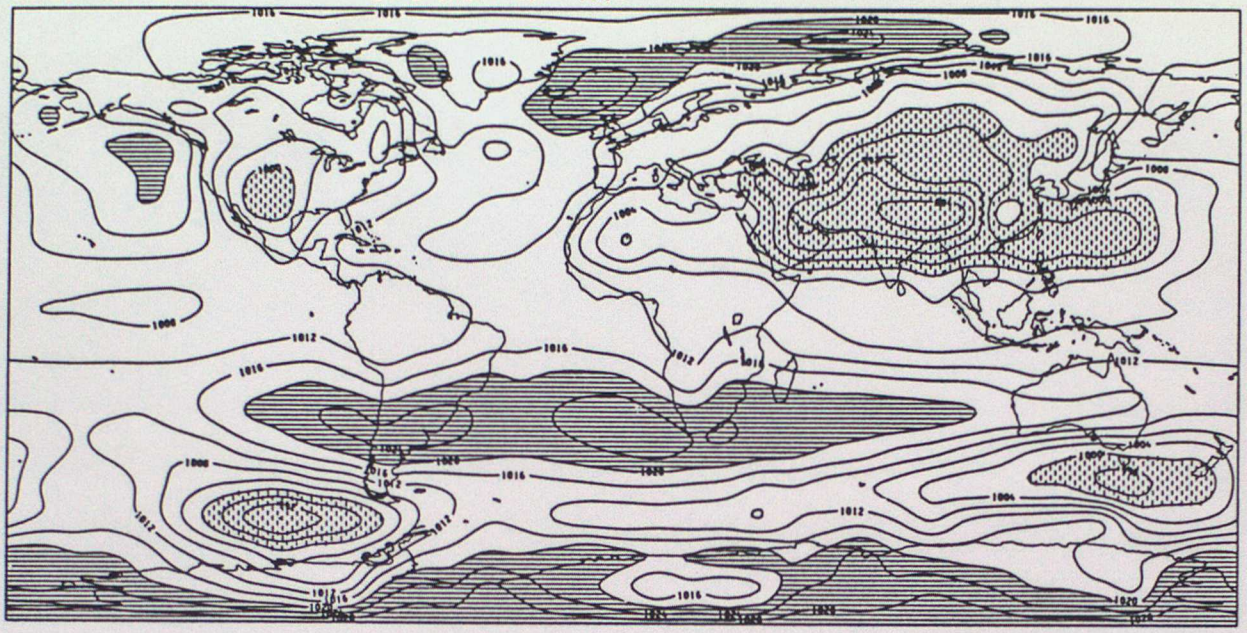

MJ25 : MEDIUM RESOLUTION JULY INTEGRATION
WITH 25*K DIFFUSION CONSTANT PMSL
AVERAGE FROM 0Z ON DAY 31 TO 0Z ON DAY 60
LEVEL: SEA LEVEL EXPERIMENT NO.: 1248

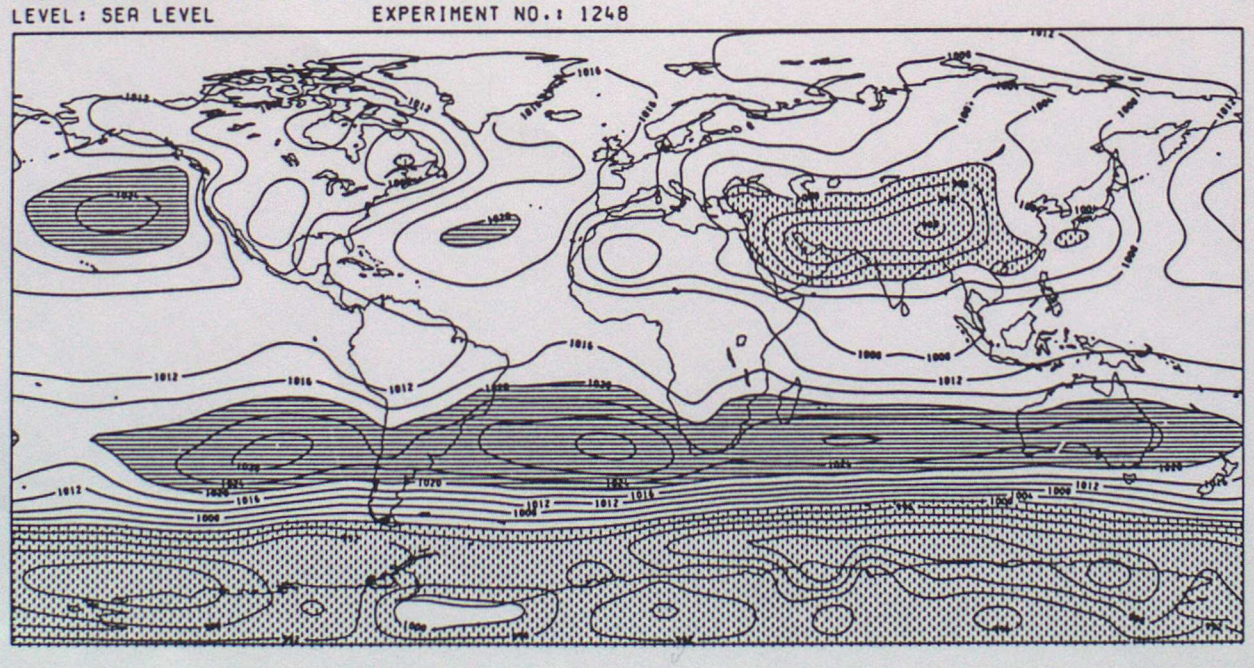

Figure 15

SCHUTZ AND GATES CLIMATOLOGICAL DATA FOR JULY
PMSL
AVERAGE FROM 0Z ON 1/7 DAY 182 TO 0Z ON 31/7 DAY 212
LEVEL: SEA LEVEL

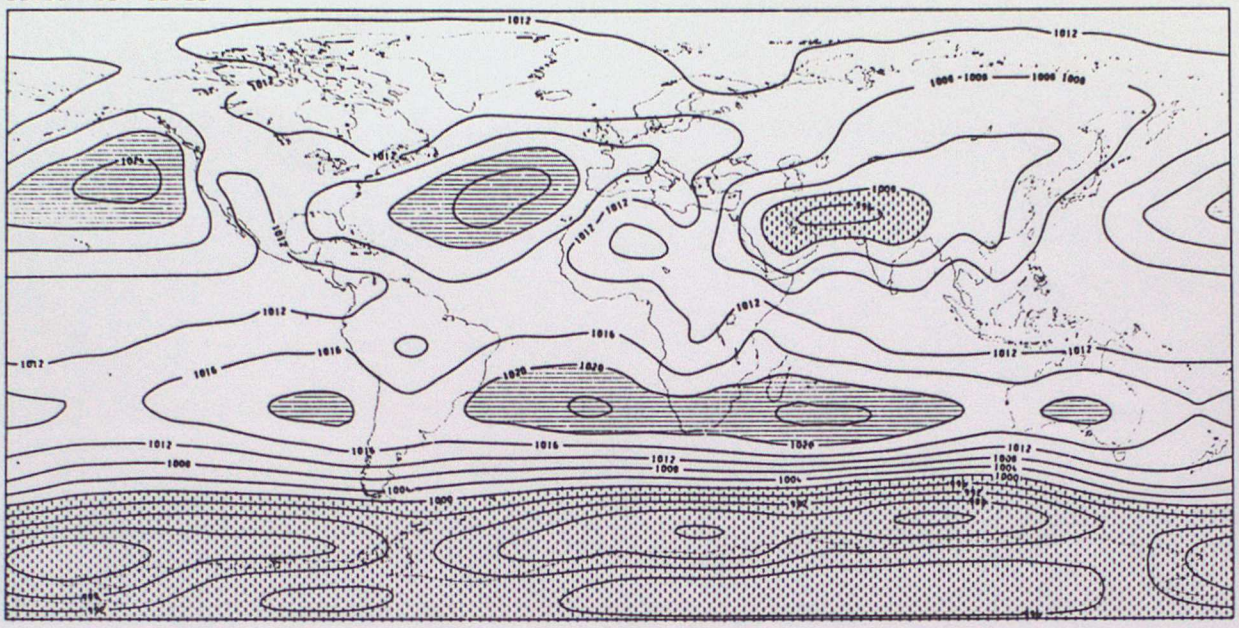

Figure 16

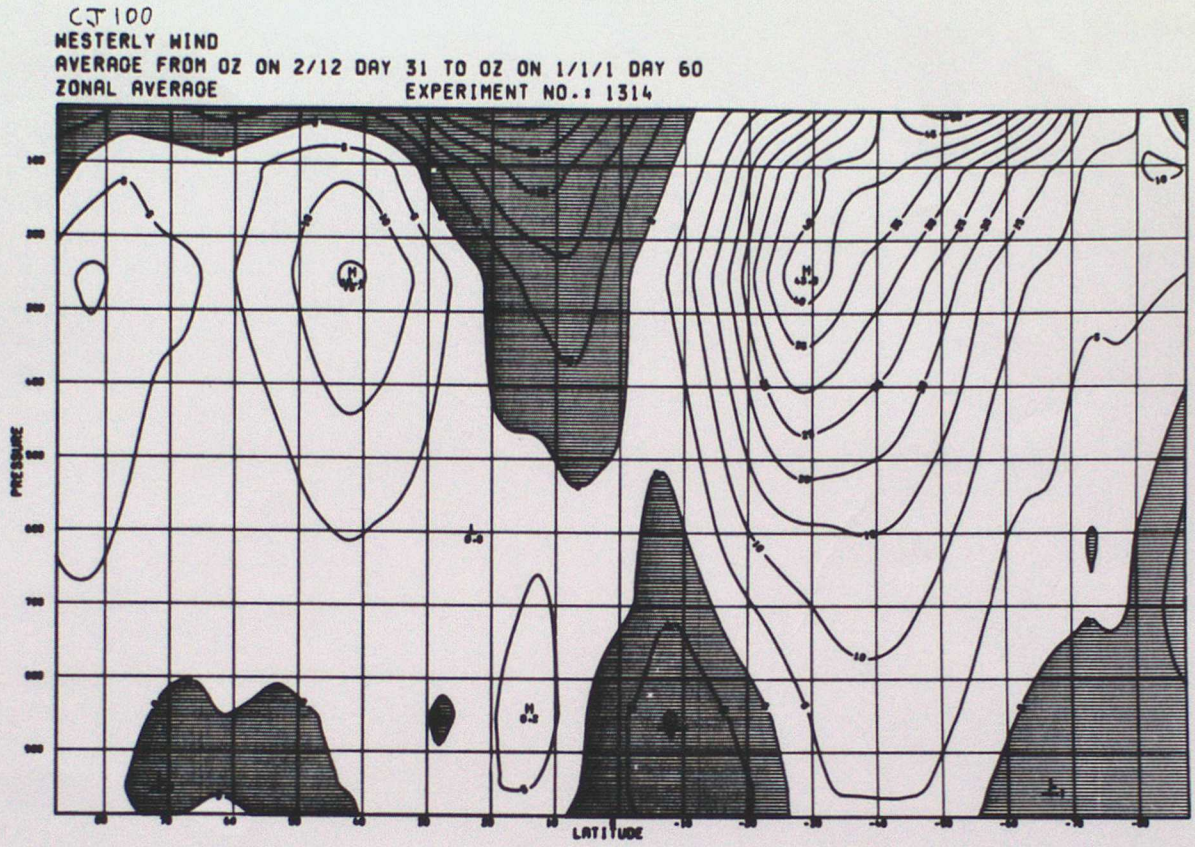
CJ100
WESTERLY WIND
AVERAGE FROM 0Z ON 2/12 DAY 31 TO 0Z ON 1/1/1 DAY 60
ZONAL AVERAGE
EXPERIMENT NO.: 1314
PRESSURE
LATITUDE

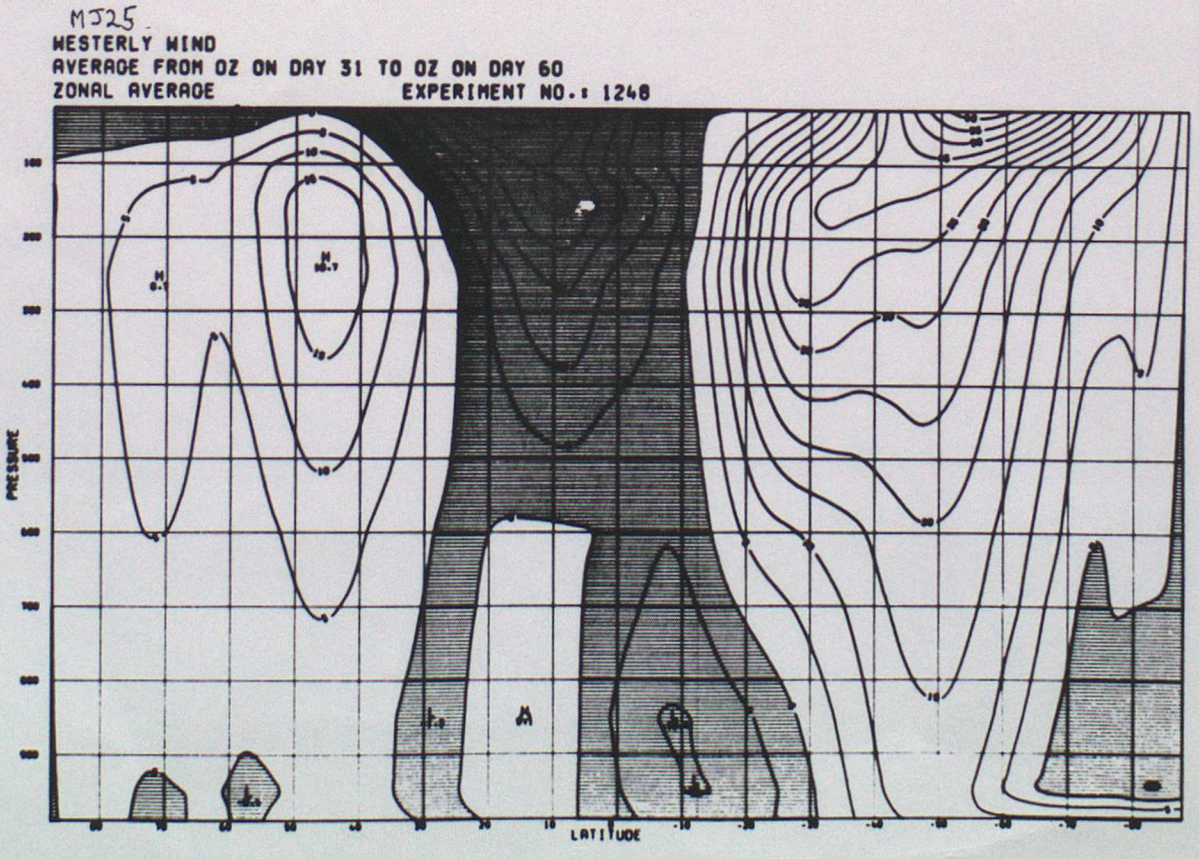
MJ25
WESTERLY WIND
AVERAGE FROM 0Z ON DAY 31 TO 0Z ON DAY 60
ZONAL AVERAGE
EXPERIMENT NO.: 1248
PRESSURE
LATITUDE

Figure 17

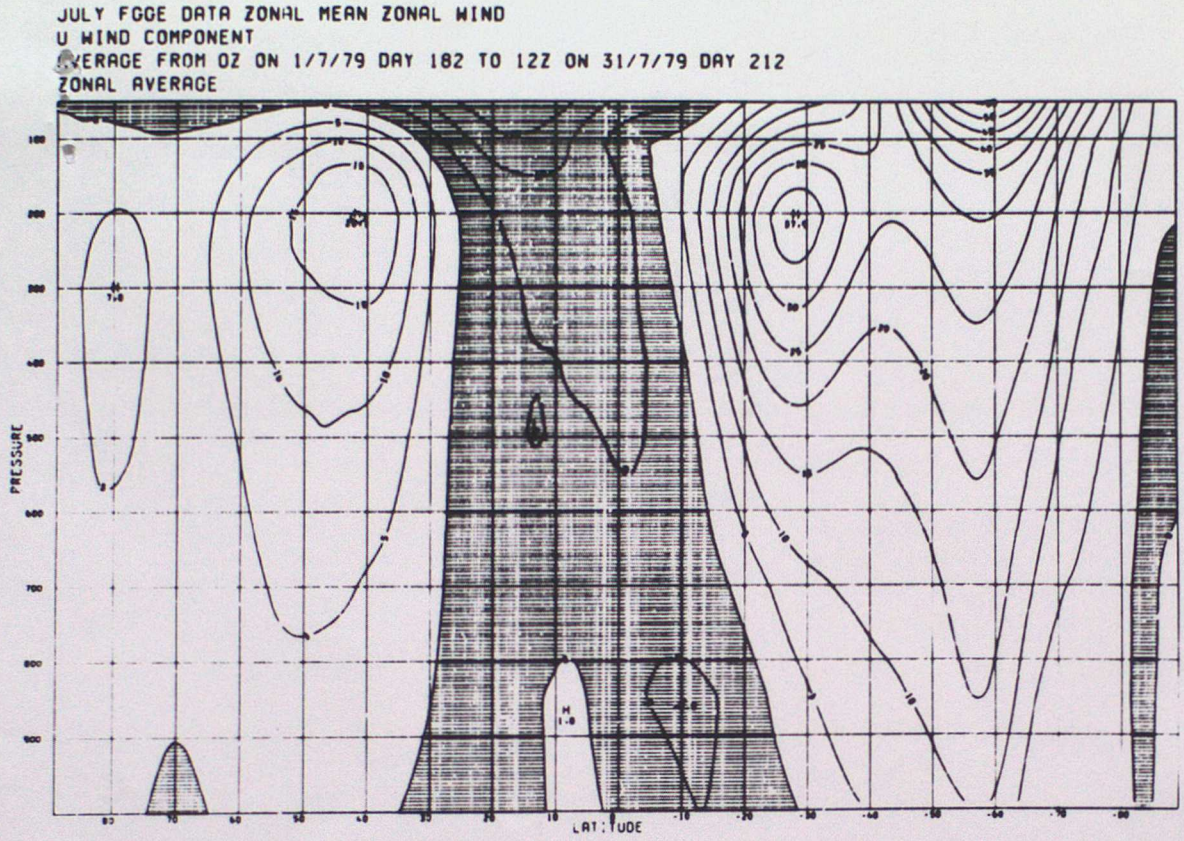
JULY FGGE DATA ZONAL MEAN ZONAL WIND
U WIND COMPONENT
VERAGE FROM OZ ON 1/7/79 DAY 182 TO 12Z ON 31/7/79 DAY 212
ZONAL AVERAGE
PRESSURE
LATITUDE

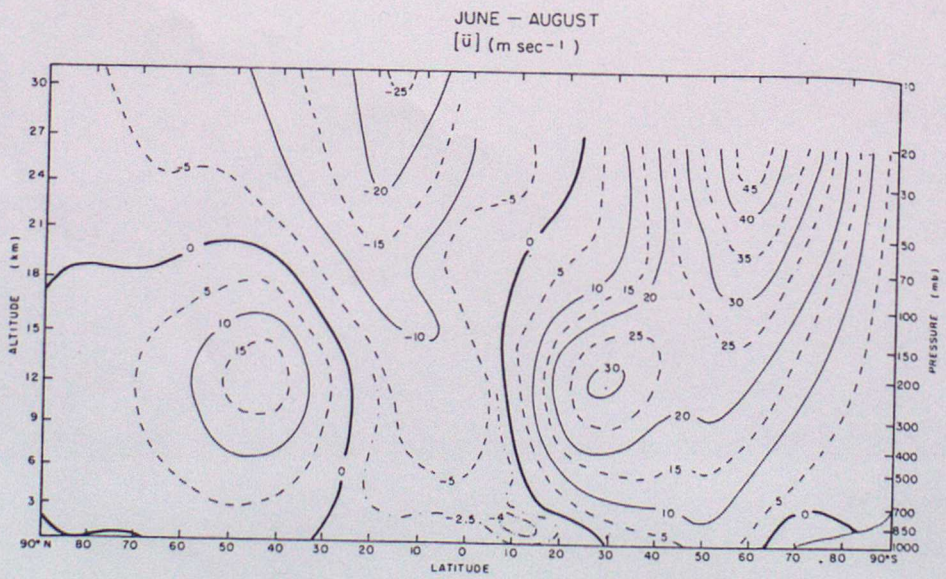
JUNE — AUGUST
[ū] (m sec⁻¹)
ALTITUDE (km)
PRESSURE (mb)
LATITUDE
90°N
90°S

Figure 18

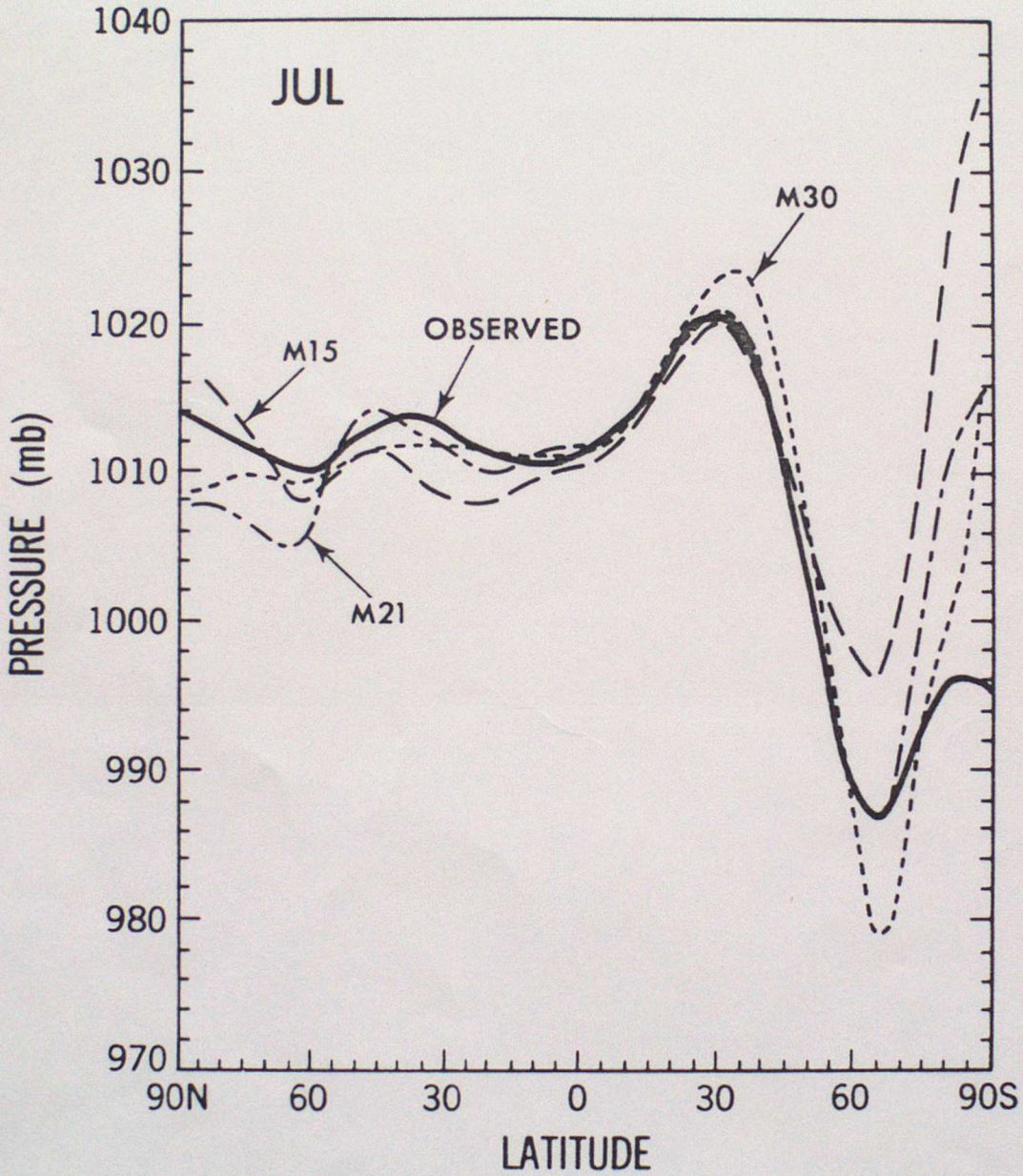

Latitudinal distributions of the July zonal mean sea level pressure (mb) for the M15, M21 and M30 spectral models and as observed (Crutcher and Meserve, 1970, and Taljaard *et al.*, 1969).

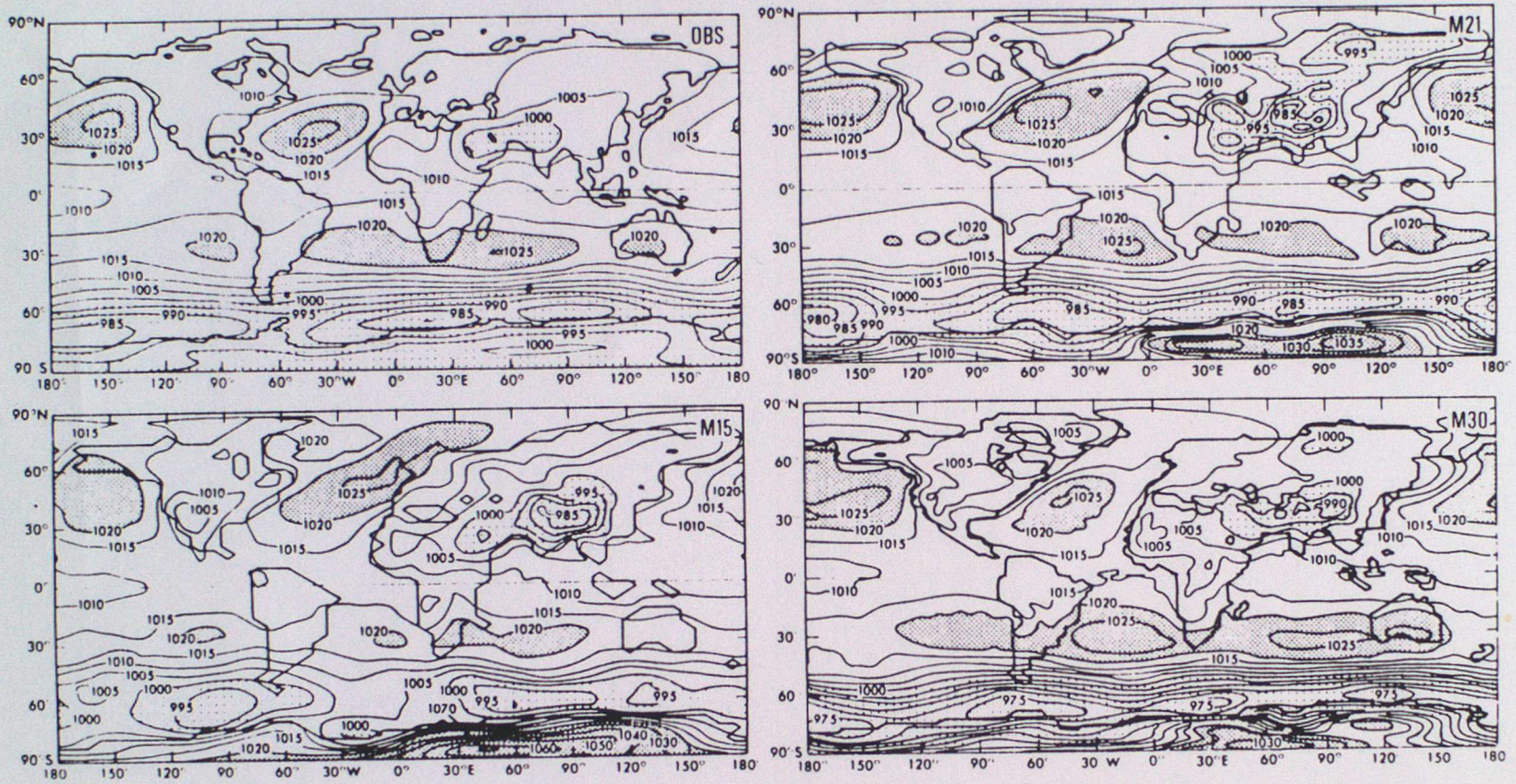

Geographical distributions of the July mean sea level pressure (mb) for the M15, M21 and M30 spectral models and observed (Crutcher and Meserve, 1970, and Taljaard *et al.*, 1969).